Physics – Uspekhi **49** (5) 441 – 467 (2006)

REVIEWS OF TOPICAL PROBLEMS PACS numbers: **74.20.–z**, 74.20.Mn, **74.72.–h**

Superconductivity of repulsive particles

V I Belyavsky, Yu V Kopaev

DOI: 10.1070/PU2006v049n05ABEH006037

Contents

Abstract. **Antiferromagnetic correlations in superconducting cuprates can lead to the mirror nesting of Fermi contour segments near saddle points of the electron spectrum and to a logarithmic singularity of the scattering amplitude for a large pair momentum. The Coulomb potential defined within a kinematically allowed region allows a negative eigenvalue, which provides superconducting pairing and weakly decaying, quasistationary, large-momentum pair states. The Ginzburg – Landau equations for the two-component superconducting order parameter provide pairs of coupled particles and pairs of coupled orbital current circulations, which explains the fundamental cuprate properties such as strong and weak pseudogaps, the superconducting transition temperature, the diamagnetic pseudogap state, and details of the isotope effect. A quantum critical point and a transition of two superconducting phases, one of which displays superconductivity with current circulations, are predicted.**

V I Belyavsky, Yu V Kopaev Lebedev Physics Institute, Russian Academy of Sciences, Leninskii prosp. 53, 119991 Moscow, Russian Federation
Tel. (7-495) 135 74 41, (7-495) 132 05 38
E-mail: kopaev@sci.lebedev.ru, vib@box.vsi.ru

Received 13 January 2006, revised 26 January 2006
Uspekhi Fizicheskikh Nauk **176** (5) 457 – 485 (2006)
Translated by M V Tsaplina; edited by A M Semikhatov

1. Introduction

In the two decades following the discovery of high-temperature cuprate superconductivity [1], a considerable amount of experimental data has been accumulated testifying to the specific behavior of these compounds in the superconducting and normal states.

The basic structural element of layered cuprate compounds is represented by copper – oxygen planes, the atomic layers between which play the role of reservoirs supplying (under hole or electron doping of the parent compound) excessive (with a concentration x) charge carriers to these planes. Parent cuprates are quasi-two-dimensional (2D) antiferromagnetic insulators with the forbidden band of about 2 eV, whose occurrence is due to sufficiently strong electron correlations [2].

It follows from the Knight shift experiments [3] that in the superconducting state, electrons form singlet pairs similar to Cooper pairs [4] in conventional superconduc-

tors described by the Bardeen – Cooper – Schrieffer (BCS) theory [5].

Superconductivity is only one of the manifestations of the rich phase diagram of cuprates, and describing the superconducting phase transition requires taking the competition and coexistence of different ordered states into account [6 – 9]. In this respect, cuprates differ notably from conventional superconductors, in which the superconducting state is a result of the instability of a normal Fermi liquid under Cooper pairing [10].

The microscopic mechanism of superconducting pairing in cuprates remains unclear. The strong electron correlations and spin antiferromagnetism of the parent compound allow assuming that this mechanism can differ from the traditional electron attraction due to the electron – phonon interaction (EPI), which is suggested by the unusual symmetry of the superconducting energy gap [11 – 14].

The on-site Coulomb correlations in a 2D electron cuprate system, which in fact forbid a double occupation of copper atom lattice sites in cuprate planes, are an obvious cause of the spin antiferromagnetism of parent compounds. The screened Coulomb repulsion, which has a finite range of action, also induces sufficiently strong on-site correlations and may be a dominant interaction leading to a superconducting pairing of charge carriers. Hence, the same interaction can occur in an insulator and a superconducting pairing channel. It is therefore natural to assume that the screened Coulomb repulsion is precisely the interaction underlying cuprate physics and allowing a unified description of the superconducting and normal states [15].

In this review, we present a concept of the superconducting pairing from Coulomb repulsion and consider the ensuing possibility of qualitatively interpreting experiments that are crucial for cuprates.

2. Phase diagram of cuprates

The phase diagram [16, 17] typical of cuprates is shown in Fig. 1. Increasing the temperature leads to an increase in the thermal disorder and to a phase transition from the antiferromagnetic to the paramagnetic phase at the Néel temperature T_N. Doping induces a T_N-lowering increase in the disorder in the structure of chemical bonds in cuprate planes. The long-range antiferromagnetic order at $T = 0$ already vanishes at the level of hole doping $x_N \approx 0.03$, whereas the short-range order survives in a vast region of the phase diagram for $x > x_N$.

Superconductivity in cuprates occurs upon doping of the parent compound and exists in a limited carrier concentration range $x_* < x < x^*$. The ranges $x < x_{opt}$ and $x > x_{opt}$, where x_{opt} is the optimum doping level corresponding to the maximum superconducting phase transition temperature, are conventionally called the underdoped and overdoped states, respectively. As the temperature increases, the overdoped cuprates move from the superconducting to the metallic state with a Fermi surface that degenerates into a Fermi contour because of the 2D anisotropy.

The energy band in which the Fermi level is located occurs from the electron states of atoms in cuprate planes, weakly bounded through charge reservoirs [18]. Hence, in the normal phase, the Fermi contour has properties that are universal for all cuprates. A considerable part of the contour belongs to an extended neighborhood of the saddle point of the dispersion law [19, 20]. As the hole doping increases, the closed Fermi

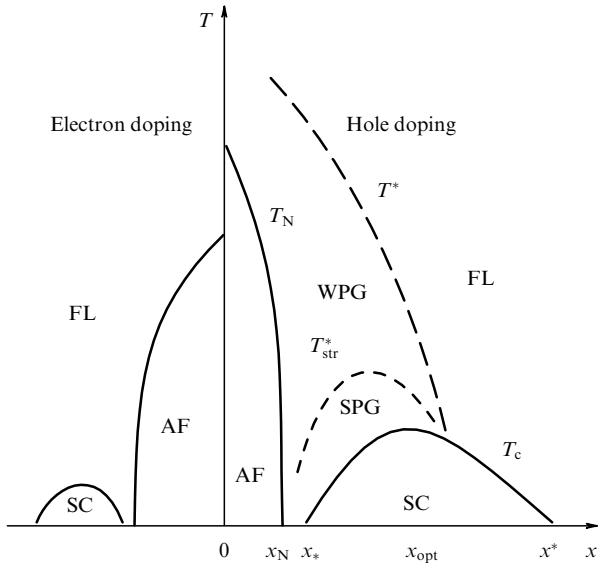

Figure 1. Schematic phase diagram of cuprate compounds. Regions of the Fermi-liquid (FL) behavior and of the antiferromagnetic (AF) and superconducting (SC) phases, and also the weak pseudogap (WPG) and strong pseudogap (SPG) regions are shown. The diagram unifies the electron and hole doping, even though both these possibilities are not realized for one and the same parent compound.

contour approaches the saddle point and passes through it at a certain concentration x_t. The topological center of the Fermi contour then shifts by the vector $\mathbf{Q} = (\pi/\bar{a}, \pi/\bar{a})$, where $\bar{a}$ is the spacing between neighboring copper atoms in the cuprate plane. For $x > x_t$, a closed Fermi contour restricts the electron occupation region [21].

In underdoped compounds, in a temperature range $T_c < T < T^*$, the Fermi contour turns out to be discontinuous and consists of arcs centered at the diagonals of the 2D Brillouin zones [22]. A pseudogap occurs instead of the disappearing parts of the Fermi contour [10, 16, 17, 23], and superconductivity occurs at the critical temperature T_c not from the metallic state of a normal Fermi liquid but from the pseudogap state. Various versions now exist concerning the origin of this pseudogap state. The arc length of the Fermi contour decreases to zero as the temperature decreases from T^* to the superconducting transition temperature T_c.

The upper temperature boundary $T^*(x)$ of the weak pseudogap [17], below which some physical properties show anomalies, is not manifested as a phase transition line and significantly exceeds T_c in strongly underdoped cuprates. Immediately above $T_c(x)$, the strong pseudogap region [17, 24] is limited from above by a temperature $T^*_{str}(x)$ of the same scale as $T_c(x)$. Diamagnetic fluctuations and the anomalous Nernst effect are observed in this region, which may be due to vortex excitations. There are grounds to believe that the pseudogap extends even into the region of extremely weak doping, $x < x_*$ [27].

3. Superconductivity upon repulsion

Taking the Coulomb repulsion into account in the framework of the EPI mechanism of superconductivity has shown [28] that the superconducting pairing requires the effective EPI coupling constant $|V|$ to exceed the Coulomb energy U_C not averaged over the Brillouin zone and its logarithmically

weakened value to be

$$|V| > \frac{U_C}{1 + g_F U_C \ln(E_F/\hbar\omega_D)}\,, \tag{1}$$

where g_F is the density of states at the Fermi level E_F and $\hbar\omega_D$ is the Debye energy, which determines the energy scale of the EPI region of electron attraction near the Fermi surface (the dynamically allowed region). The energy gap parameter in the Bogolyubov – Tolmachev – Shirkov (BTS) model [28], defined in the entire Brillouin zone, reverses sign at the boundary of the dynamically allowed region, which explains the weakened effect of the Coulomb repulsion upon superconducting pairing. We note that a formal narrowing of the dynamically allowed region ($\omega_D \to 0$), for instance, as a result of the intersection of the line of zero values of the energy gap parameter with the Fermi surface, lifts the restriction from the effective EPI coupling constant altogether (but decreases the pre-exponential factor to zero in the expression for the pair binding energy).

The study of repulsive interaction as the mechanism of superconductivity began soon after the creation of the BCS theory. In the consideration of superconductivity of transition metals within the two-band model [29, 30], it was shown that a nontrivial solution of the energy gap equation appears in the case of repulsion when the Suhl inequality holds:

$$U_{11}U_{22} - U_{12}U_{21} < 0\,, \tag{2}$$

where $U_{nn'}$ are intraband (for $n = n'$) and interband (for $n \neq n'$) matrix elements of the interaction operator.

Kohn and Luttinger [31] showed that superconducting pairing can be caused by the repulsive potential $U(\mathbf{r})$, which, under the condition

$$\int U(\mathbf{r})\,\mathrm{d}V > 0\,, \tag{3}$$

where the integration ranges the entire space, assumes negative values in a finite region of real space. Such a property is inherent (see, e.g., Ref. [31]) in the screened Coulomb potential in a degenerate electron system, which shows Friedel oscillations owing to the presence of an occupied Fermi sphere. The general conditions for the appearance of bound (and quasistationary) states in the given potential $U(r)$ are determined by Levinson's theorem [32].

As noted by Landau [33], the superconducting pairing due to repulsion takes place if at least one partial scattering length in the expansion of the pairing potential in spherical harmonics is negative. The symmetry of the energy gap $\Delta(\mathbf{k})$ as a function of the momentum $\mathbf{k}$ of the relative motion of the pair is determined by a linear combination of spherical harmonics with a given value of the orbital angular momentum l [34]. We note that condition (3) excludes the possibility of pairing in the case of repulsion with $l = 0$ (which corresponds to the s-wave symmetry of the order parameter).

The Kohn singularity of the permittivity of a degenerate electron system [35], which results in Friedel oscillations of the effective repulsive potential

$$U(r) \sim r^{-3}\cos(2k_F r)\,,$$

leads to the inevitable occurrence of negative partial scattering lengths among those with $l \neq 0$, corresponding to effective attraction [31]. For the model of a weakly nonideal electron gas with screened Coulomb repulsion, it is shown [36] that all the partial scattering lengths with $l \neq 0$ are negative, which results in the superconducting instability in the pairing channel with zero total pair momentum.

Singlet superconducting pairing in cuprates corresponds to even l, and therefore, in the simplest case, the pairing due to repulsion results in a d-wave symmetry of the energy gap (which vanishes at four points of the Fermi contour and reverses sign under rotation by $\pi/2$ in the 2D momentum space). The one-dimensional irreducible representation B_{1g} of the point symmetry group of a cuprate plane corresponds to a gap with the d-wave symmetry.

The trivial irreducible representation A_{1g} can refer not only to an isotropic gap with the s-wave symmetry but also to a more complicated dependence of $\Delta(\mathbf{k})$ on the direction in the momentum space [13, 14], for instance, to an anisotropic s-wave symmetry when $\Delta(\mathbf{k})$ has no zeros on the Fermi contour, or to an extended s-wave symmetry when $\Delta(\mathbf{k})$ has eight zeros grouped in pairs ($s + g$-symmetry [13, 14]). In the case of the s-wave symmetry, the gap does not change sign under rotation by $\pi/2$.

For an interaction satisfying the Kohn – Luttinger condition, the equation for $\Delta(\mathbf{k})$ has a sign-alternating solution in momentum space. It is only in this case that competing contributions of opposite signs can occur in this equation, and the prevalence of the negative contribution can be guaranteed if $U(\mathbf{k}) > 0$, where $U(\mathbf{k})$ is the Fourier transform of the pairing potential $U(\mathbf{r})$. This means that according to the Suhl inequality, the contribution of particle scattering between regions of momentum space with different signs of $\Delta(\mathbf{k})$ prevails over the contribution of scattering between regions with the same sign of $\Delta(\mathbf{k})$. Hence, experimental evidence of the existence of energy-gap zeros in superconducting cuprates with hole doping is an argument in favor of the microscopic mechanism of superconductivity in these compounds, based on the pairing repulsion.

Superconducting paring in a channel with a nonzero orbital angular momentum leads to rather low $T_c \sim \exp\{-(2l)^4\}$ values [31]. The dimensionless coupling constants determining the exponential dependence of T_c for Coulomb repulsion and EPI-induced attraction are estimated similarly by the order of magnitude, $w_C \sim w_{ph} \sim 1$, while the pre-exponential factors are essentially different, the characteristic Coulomb energy ε_0 exceeding the Debye energy $\hbar\omega_D$ by several orders of magnitude. However, in contrast to the EPI mechanism leading to an isotropic s-wave order parameter [37], the pairing repulsion inevitably corresponds to an energy gap with zeros at several points of the Fermi contour.

The Friedel oscillations of a screened Coulomb potential occur owing to a rather weak Kohn singularity of screening [35], and therefore such a potential, as well as the strongly anisotropic repulsion due to antiferromagnetic spin fluctuations [38, 39], corresponds to a small coupling constant $w \ll 1$ and, accordingly, to low superconducting transition temperatures [40]. In the 2D electron system of cuprate planes, this singularity is enhanced, but because of developed fluctuations the phase transition can [17] acquire features of the Berezinski – Kosterlitz – Thouless (BKT) transition [33].

4. Pairing with large momentum

Yang showed [41] that the states formed of singlet pairs localized on one crystal lattice site (η-pairing) are eigen-

states, but are simultaneously metastable states of the simple Hubbard model for the total pair momenta $\mathbf{K} = 0$ and $\mathbf{K} = (\pi, \pi)$. In the Penson – Kolb – Hubbard model [42], i.e., an extended Hubbard model allowing repulsive-pair hopping between neighboring sites, a state in the form of a superconducting condensate of η_π-pairs with the large momentum $\mathbf{K} = (\pi, \pi)$ can become the ground state [43, 44] competing successfully with the superconducting condensate state of η_0-pairs with the momentum $\mathbf{K} = 0$ and with energetically close insulating states [44].

In superconducting pairing with a nonzero pair momentum $\mathbf{K}$, a spatially inhomogeneous state similar to the Fulde – Ferrell – Larkin – Ovchinnikov (FFLO) state [45, 46] occurs in weakly ferromagnetic superconductors. For pairs with $\mathbf{K} \neq 0$, the regions of momentum space accessible for pairing of both electrons and holes contract considerably, with the result that the FFLO state corresponds to a pair condensate with a momentum close to zero and a long-wave order parameter modulation.

The Fermi contour determined by the equation $\varepsilon(\mathbf{q}) = \mu$, where μ is the chemical potential, separates the momentum space into regions of occupied and vacant states. In superconducting pairing, both particles must be located in one of these regions, and this condition restricts the domain of definition of the momenta $\mathbf{k}_+$ and $\mathbf{k}_-$ of pair-constituting particles [or, for a given $\mathbf{k}_+ + \mathbf{k}_- = \mathbf{K}$, the domain of definition of the relative motion momentum $\mathbf{k} = (\mathbf{k}_+ - \mathbf{k}_-)/2$] [47].

Figure 2a shows how the kinematically allowed region Ξ occurs in the case of the two-dimensional isotropic dispersion law when the Fermi contour is a circle with the radius equal to the Fermi momentum k_{F}. For $\mathbf{K} \neq 0$, the region Ξ does not coincide with the Brillouin zone. The sum of kinetic energies of a pair of particles, counted from the chemical potential,

$$2\xi(\mathbf{k}) = \varepsilon\left(\frac{\mathbf{K}}{2} + \mathbf{k}\right) + \varepsilon\left(\frac{\mathbf{K}}{2} - \mathbf{k}\right) - 2\mu\,, \tag{4}$$

vanishes not on the entire Fermi contour as in the case where $\mathbf{K} = 0$ [when $\xi(\mathbf{k})$ has the meaning of the kinetic energy of a particle or a hole with respect to the Fermi level] but, generally speaking, only at some of its points (the intersection points, marked in Fig. 2a, of circles displaced relative to each other by the vector $\mathbf{K}$). For large $\mathbf{K}$, the region Ξ is comparatively small, and so are the momenta of the relative motion. On the contrary, for $\mathbf{K} = 0$, the momenta of the relative motion, coincident with the momenta of pair-constituting particles, are large: $k \approx k_{\mathrm{F}}$.

Singlet pairing with $\mathbf{K} \neq 0$ can be described by the Hamiltonian $\hat{H} = \hat{H}_0 + \hat{V}$, with the kinetic energy operator

$$\hat{H}_0 = \sum_{\mathbf{k}} \varepsilon(\mathbf{k}_+)\hat{c}^{\dagger}_{\mathbf{k}_+}\hat{c}_{\mathbf{k}_+} + \sum_{\mathbf{k}} \varepsilon(\mathbf{k}_-)\hat{c}^{\dagger}_{\mathbf{k}_-}\hat{c}_{\mathbf{k}_-} \tag{5}$$

and the potential energy operator

$$\hat{V} = \sum_{\mathbf{k}\,\mathbf{k}'} U(\mathbf{k} - \mathbf{k}')\hat{c}^{\dagger}_{\mathbf{k}_+}\hat{c}^{\dagger}_{\mathbf{k}_-}\hat{c}_{\mathbf{k}'_-}\hat{c}_{\mathbf{k}'_+}\,, \tag{6}$$

where summation over momenta $\mathbf{k}$ and $\mathbf{k}'$ of the relative motion is performed for a given total momentum $\mathbf{K}$. Here, $\mathbf{k}_\pm = \mathbf{K}/2 \pm \mathbf{k}$, $\mathbf{k}'_\pm = \mathbf{K}/2 \pm \mathbf{k}'$, $\hat{c}^{\dagger}_{\mathbf{k}_\pm}$ and $\hat{c}_{\mathbf{k}_\pm}$ are the creation and annihilation operators of a particle with momentum $\mathbf{k}_\pm$ and spin $\pm 1/2$, and $U(\mathbf{k} - \mathbf{k}')$ is the matrix element of the pairing interaction energy.

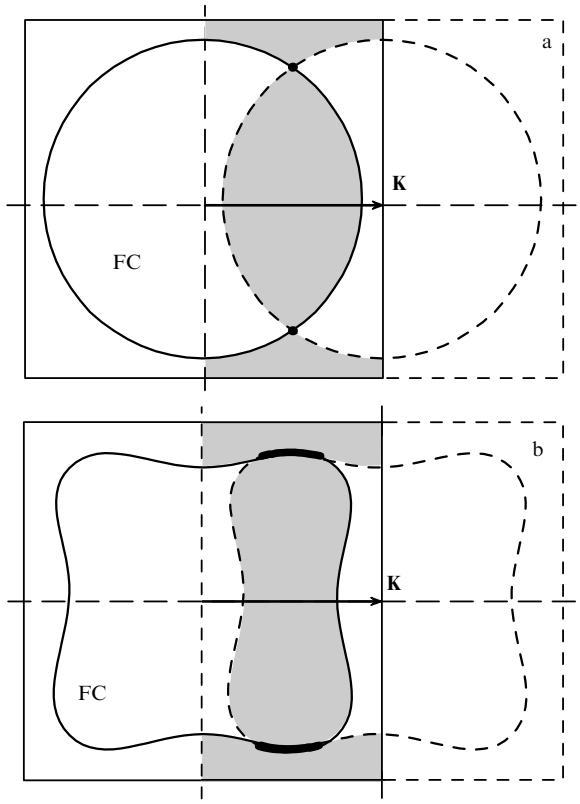

Figure 2. Kinematically allowed region (shaded) inside the crystallographic Brillouin zone for pairs of particles and holes with a total momentum $\mathbf{K}$. (a) Isotropic Fermi contour (FC) with two marked points pertaining to the kinematically allowed region; (b) Fermi contour with mirror nesting. The thick line shows finite regions of the Fermi contour within the kinematically allowed region.

One can introduce anomalous averages $\langle \hat{c}_{\mathbf{k}_+}\hat{c}_{\mathbf{k}_-} \rangle$ corresponding to singlet pairing with the total momentum $\mathbf{K}$; having found the energy gap parameter depending on the momentum of the relative motion of the pair [48],

$$\Delta(\mathbf{k}) = \sum_{\mathbf{k}'} U(\mathbf{k} - \mathbf{k}')\,\langle \hat{c}_{\mathbf{k}'_+}\hat{c}_{\mathbf{k}'_-} \rangle\,, \tag{7}$$

one then diagonalizes the Hamiltonian $\hat{H}$ using the Bogolyubov transformation. This defines the new Fermi quasiparticle operators relating the creation and annihilation operators of particles with momenta $\mathbf{k}_+$ and $\mathbf{k}_-$ and opposite spins:

$$\hat{c}_{\mathbf{k}_+} = u_{\mathbf{k}_+}\hat{b}_{\mathbf{k}_+} + v_{\mathbf{k}_-}\hat{b}^{\dagger}_{\mathbf{k}_-}\,, \qquad \hat{c}_{\mathbf{k}_-} = u_{\mathbf{k}_-}\hat{b}_{\mathbf{k}_-} - v_{\mathbf{k}_+}\hat{b}^{\dagger}_{\mathbf{k}_+}\,. \tag{8}$$

The coherence factors found in diagonalizing the Hamiltonian are given by

$$\begin{aligned} u_{\mathbf{k}_\pm} &= \sin\vartheta \exp\left(\frac{\mathrm{i}\Phi}{2}\right) \exp\left(\pm\mathrm{i}\varphi_\pm\right), \\ v_{\mathbf{k}_\pm} &= \cos\vartheta \exp\left(\frac{\mathrm{i}\Phi}{2}\right) \exp\left(\mp\mathrm{i}\varphi_\mp\right), \end{aligned} \tag{9}$$

where Φ, φ_+, and φ_- are arbitrary phases and the parameter ϑ is determined by the relation $\tan 2\vartheta = \left|\Delta(\mathbf{k})\right| / \xi(\mathbf{k})$.

The anomalous average assumes the form

$$\langle \hat{c}_{\mathbf{k}_+}\hat{c}_{\mathbf{k}_-} \rangle = -\sin 2\vartheta \exp\left(\mathrm{i}\Phi\right) \frac{\Theta(\mathbf{k}; T)}{2}\,, \tag{10}$$

where $\Theta(\mathbf{k};T) = 1 - n_{\mathbf{k}_+} - n_{\mathbf{k}_-}$, with $n_{\mathbf{k}_\pm}$ being the distribution function of quasiparticles with the momentum $\mathbf{k}_\pm$ and spin $\pm 1/2$. The energy gap parameter $\Delta(\mathbf{k}) = |\Delta(\mathbf{k})| \exp(\mathrm{i}\Phi)$ determines the internal (associated with the relative motion) structure of a pair with the momentum $\mathbf{K}$ and satisfies the self-consistency equation

$$\Delta(\mathbf{k}) = -\frac{1}{2}\sum_{\mathbf{k}'} \frac{U(\mathbf{k}-\mathbf{k}')\,\Delta(\mathbf{k}')}{\sqrt{\xi^2(\mathbf{k}') + |\Delta(\mathbf{k}')|^2}}\,\Theta(\mathbf{k}';T)\,. \tag{11}$$

The anomalous average in (10) and the parameter $\Delta(\mathbf{k})$ are determined up to a phase factor, where the phase can be represented as $\Phi = \Phi_c + \beta$, where the phase Φ_c refers to the center-of-mass motion and is related to the establishment of phase coherence in the system of pairs at temperatures below T_c and β determines the internal structure of the pair associated with the relative motion.

The contribution, diagonal in quasiparticle operators, to the transformed Hamiltonian determines two branches of the quasiparticle dispersion law [48]

$$E_\pm(\mathbf{k}) = E(\mathbf{k}) \pm \frac{\varepsilon(\mathbf{k}_+) - \varepsilon(\mathbf{k}_-)}{2}\,, \tag{12}$$

where

$$E(\mathbf{k}) = \sqrt{\xi^2(\mathbf{k}) + |\Delta(\mathbf{k})|^2}\,. \tag{13}$$

The gap in the quasiparticle spectrum occurs under the mirror nesting condition [49]

$$\varepsilon\left(\frac{\mathbf{K}}{2} + \mathbf{k}\right) = \varepsilon\left(\frac{\mathbf{K}}{2} - \mathbf{k}\right), \tag{14}$$

which, in the case of Cooper pairing with $\mathbf{K} = 0$, holds trivially due to the general property of the dispersion law $\varepsilon(-\mathbf{q}) = \varepsilon(\mathbf{q})$.

For $\mathbf{K} \neq 0$, condition (14) is normally satisfied only at some points of the Fermi contour (Fig. 2a), and therefore no logarithmic singularity is present in (11). But for a special form of the electron dispersion law, the condition can hold on separate finite regions of the Fermi contour (Fig. 2b). In this case, because $\xi(\mathbf{k}) = 0$ on the Fermi contour, the self-consistency equation becomes singular and, if the kernel of this equation $U(\mathbf{k}-\mathbf{k}')$ allows a bound state, the equation already has a solution for arbitrarily low pairing interaction intensity [50]. When the mirror nesting condition is satisfied approximately, the logarithmic singularity is smoothed and the effective coupling constant must exceed a certain threshold value for relative motion of the bound state of the pair to occur [51].

The perfect mirror nesting condition (14) uniquely defines the momentum $\mathbf{K}$ of pairs precipitating to the superconducting condensate. This momentum corresponds to the free-energy minimum (the maximum energy of superconducting condensation [49]), which also determines the momentum $\mathbf{K}$ (which may be incommensurate) when condition (14) is satisfied approximately.

Equation (14) specifies the locus of points in the momentum space of the relative motion to which the quasiparticle spectrum $E(\mathbf{k})$ with an anisotropic energy gap $2|\Delta(\mathbf{k})|$ corresponds. Another equation, $\nabla_k E(\mathbf{k}) = 0$, specifies the locus of points at which the quasiparticle group velocity becomes zero in the case of mirror nesting. Because of the energy gap parameter anisotropy, the corresponding line of the quasiparticle excitation energy minima does not coincide with the Fermi contour [52] as it would in the case of s-wave pairing.

If the mirror nesting condition is satisfied, the occupation numbers $n_{\mathbf{k}_\pm}$ are equal to unity or zero at $T = 0$ and $\Delta \to 0$ if the momenta $\mathbf{k}_\pm$ are inside or outside the Fermi contour. Hence, $\Theta(\mathbf{k};0) = 1$ whenever the momenta $\mathbf{K}/2 \pm \mathbf{k}$ of both particles constituting a pair with the momentum $\mathbf{K}$ are inside or outside the Fermi contour, and $\Theta(\mathbf{k};0) = 0$ otherwise. This condition describes the kinematically allowed region over which the summation is performed in (11). At a nonzero temperature, the Fermi step in the distribution function of quasiparticles is smeared, and therefore $\Theta(\mathbf{k};T) \lesssim 1$ within the kinematically allowed region and $\Theta(\mathbf{k};T) \ll 1$ outside it at sufficiently low temperatures.

The mirror nesting of the Fermi contour makes the channel of superconducting (particle–particle) pairing effective without affecting the channel of insulating (particle–hole) pairing, in which a logarithmic singularity does not occur. Therefore, the mirror nesting, in contrast to the ordinary nesting, cannot cause a radical reconstruction of the phonon spectrum.

5. Pairing condition in the case of repulsion

The matrix element $U(\mathbf{k}-\mathbf{k}')$ is related to the pairing potential $U(\mathbf{r})$ in real space by the Fourier transformation

$$U(\mathbf{k}-\mathbf{k}') = \int U(\mathbf{r}) \exp\left[\mathrm{i}(\mathbf{k}-\mathbf{k}')\,\mathbf{r}\right] \mathrm{d}^2 r\,. \tag{15}$$

It is taken into account here that the momenta $\mathbf{k}$ and $\mathbf{k}'$ belong to the two-dimensional momentum space. Multiplying self-consistency equation (11) by $\Delta(\mathbf{k})\,\Theta(\mathbf{k};T)/E(\mathbf{k})$ and summing over $\mathbf{k}$ leads to the relation

$$\sum_{\mathbf{k}} \frac{|\Delta(\mathbf{k})|^2\,\Theta(\mathbf{k};T)}{E(\mathbf{k})} = -\frac{1}{2}\int U(\mathbf{r})\,L(\mathbf{r})\,\mathrm{d}^2 r\,, \tag{16}$$

where the nonnegative function $L(\mathbf{r})$ is given by

$$L(\mathbf{r}) = \left|\sum_{\mathbf{k}} \frac{\Delta(\mathbf{k})\,\Theta(\mathbf{k};T)}{E(\mathbf{k})} \exp(\mathrm{i}\mathbf{k}\mathbf{r})\right|^2. \tag{17}$$

Relation (16) shows that the self-consistency equation cannot have a nontrivial solution if the effective potential $U(\mathbf{r})$ is nonnegative for all values of $\mathbf{r}$.

The self-consistency equation is a nonlinear integral Hammerstein equation with a symmetric kernel $U(\mathbf{k}-\mathbf{k}')$. The eigenfunctions and eigenvalues of the linear Hermitian operator with the kernel $U(\mathbf{k}-\mathbf{k}')$ are defined by the equation

$$\varphi_s(\mathbf{k}) = \lambda_s \sum_{\mathbf{k}'\in\Xi} U(\mathbf{k}-\mathbf{k}')\,\varphi_s(\mathbf{k}')\,. \tag{18}$$

As usual, we assume transition from summation to integration over the kinematically allowed region in which the kernel $U(\mathbf{k}-\mathbf{k}')$ is defined and which is the domain of definition of the eigenfunctions $\varphi_s(\mathbf{k})$ forming a complete orthonormal system

$$\sum_{\mathbf{k}} \varphi^*_{s'}(\mathbf{k})\,\varphi_s(\mathbf{k}) = \delta_{ss'}\,, \qquad \sum_{s} \varphi^*_s(\mathbf{k}')\,\varphi_s(\mathbf{k}) = \delta_{\mathbf{k}\mathbf{k}'}\,. \tag{19}$$

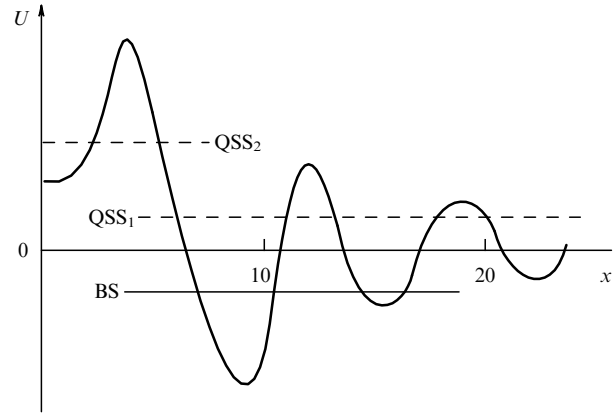

Figure 3. Schematic representation of pairing potential (20) in real space ($x = 2k_F r$). The energy levels of the bound state (BS) and two quasistationary states (QSS) that can arise in such a potential are shown.

All eigenvalues of the Hermitian operator kernel are real and form a discrete spectrum λ_n, which for a nondegenerate kernel has an accumulation point $|\lambda_n| \to \infty$ as $n \to \infty$ [53]. If the kernel $U(\mathbf{k} - \mathbf{k}')$ is the Fourier transform of an everywhere positive potential $U(r)$, then all its eigenvalues are positive. In this case, the self-consistency equation has a trivial solution only. The necessary and sufficient condition for the existence of a nontrivial solution is the presence of at least one negative eigenvalue in the spectrum of the kernel $U(\mathbf{k} - \mathbf{k}')$ [50], which may happen if $U(\mathbf{r}) < 0$ in a finite region of the real space.

Screening significantly affects the effective pairing potential of Coulomb repulsion, which, for the interaction in an empty space and in a classical electron gas (for Debye screening) corresponds to positive eigenvalues only. In a degenerate electron gas, the presence of a Fermi surface leads to a Kohn singularity in screening and, as a consequence, to the appearance of one negative eigenvalue.

In contrast to the screened Coulomb potential with a Kohn singularity at $k = 2k_F$, defined in the case of pairing with $\mathbf{K} = 0$ in the entire Brillouin zone, the matrix element $U(\mathbf{k})$ of pairing interaction with large momentum is defined in the kinematically allowed domain, which corresponds to a cutoff of $U(\mathbf{k})$ at the boundary of this domain. As a result, the effective pairing potential $U(\mathbf{r})$ in real space, which is the inverse Fourier transform of the matrix element $U(\mathbf{k})$, proves to be a sign-alternating function of its argument (Fig. 3). The effective coupling constant corresponding to such a potential considerably exceeds the constant corresponding to the screened Coulomb potential with Friedel oscillations. We note that for large momenta, the screening singularities can be due to sign reversal of the inverse permittivity [54].

The kinematically allowed region is a part of the Brillouin zone, and therefore the momentum $\mathbf{k}$ of the relative motion of a pair with momentum $\mathbf{K}$ is small because of the smallness of this region, and the matrix element of the screened Coulomb potential can be represented by first several terms of the series expansion in powers of its argument. Up to second-order terms, we have [50]

$$U(\mathbf{k} - \mathbf{k}') = \frac{U_0 r_0^2}{S}\left(1 - \frac{(\mathbf{k} - \mathbf{k}')^2 r_0^2}{2}\right), \tag{20}$$

where U_0 is the characteristic Coulomb energy, r_0 has the meaning of the screening radius, and S is the normalization area. This approximation is sufficient for a qualitative study of Coulomb pairing if the domain of definition of the momentum of relative motion, $0 \leqslant k^2 \lesssim \Xi$, is such that matrix element (20) is positive for all $\mathbf{k}$ from Ξ. This condition can be satisfied for a sufficiently strong screening, when $r_0^2 \Xi < 1$.

Matrix element (20) determines the degenerate kernel of the self-consistency equation, which has four eigenfunctions, two of which are even and the other two are odd under the transformation $\mathbf{k} \to -\mathbf{k}$ [50]. One of the even functions, sign-alternating in the region Ξ, corresponds to a negative eigenvalue, while the other three belong to positive eigenvalues. Kernel (20) is minimal (in the sense of the dimension of the linear space spanned by the kernel eigenfunctions) and leads to a negative eigenvalue under condition (3). The simplest kernel given by a positive constant in the Ξ region has a single eigenfunction $\varphi = \text{const}$ corresponding to a positive eigenvalue. Although such a kernel leads to an oscillating effective potential $U(\mathbf{r})$, the respective self-consistency equation has a trivial solution only. Therefore, the necessary condition $U(\mathbf{r}) < 0$ in a certain region of real space is not sufficient for the existence of a nontrivial solution of the self-consistency equation for pairing repulsion.

6. Single-pair problem

The bound state that occurs in the Cooper problem of two particles or holes with zero total momentum attracting in a thin dynamically restricted layer (with the energy scale $\sim \hbar\omega_D$) near the Fermi surface testifies to the instability of the ground state of the system in which all the one-particle states inside (outside) the Fermi surface are occupied (vacant). The same conclusion is suggested by the solution of the Cooper problem with a long-range attracting interaction [55] leading to a fairly involved internal structure of the pair, and by the solution of the problem of two repulsive particles with $\mathbf{K} \neq 0$ under the condition that the potential $U(\mathbf{k} - \mathbf{k}')$ has at least one negative eigenvalue and that the kinematically allowed region of the 2D electron system includes, owing to mirror nesting, finite regions of the Fermi contour [56]. Moreover, long-lived quasistationary states (QSSs) may in this case arise in the continuum of the relative motion of a pair. Such states, which manifest themselves as fluctuations of the superconducting order parameter above T_c, are incoherent pairs with different total momenta close to the momentum $\mathbf{K}$ of the superconducting condensate.

The wave function $\psi(\mathbf{k})$ of the relative motion of a pair with momentum $\mathbf{K}$ can be found from the equation [56]

$$\psi(\mathbf{k}) = G(\mathbf{k}; E) \sum_{\mathbf{k}'} U(\mathbf{k} - \mathbf{k}')\, \Theta(\mathbf{k}'; T)\, \psi(\mathbf{k}')\,, \tag{21}$$

where E is the energy of the pair counted from the chemical potential 2μ and $G(\mathbf{k}; E) = \left[E - \xi(\mathbf{k})\right]^{-1}$ is the retarded Green's function of the free relative motion.

Expanding the function $\Theta(\mathbf{k}; T)\,\psi(\mathbf{k})$ in eigenfunctions $\varphi_s(\mathbf{k})$ of the kernel $U(\mathbf{k} - \mathbf{k}')$ in Eqn (21), we can reduce this equation to a linear algebraic system for the expansion coefficients $\alpha_s(T)$:

$$\sum_{s'} \left\{\delta_{ss'} - \lambda_{s'}^{-1}\, G_{ss'}(E; T)\right\} \alpha_{s'}(T) = 0\,. \tag{22}$$

Its solvability condition

$$\det\left\{\delta_{ss'} - \lambda_{s'}^{-1}\, G_{ss'}(E; T)\right\} = 0 \tag{23}$$

allows finding the temperature-dependent energy spectrum of the relative motion of the pair. The matrix elements of the Green's function have the form

$$G_{ss'}(E;T) = \sum_{\mathbf{k}} \varphi_s^*(\mathbf{k})\, G(\mathbf{k};E)\, \Theta(\mathbf{k};T)\, \varphi_{s'}(\mathbf{k})\,. \tag{24}$$

In general, Eqns (22) represent an infinite system solved (using the standard technique of approximate solution) by replacing the nondegenerate kernel with a degenerate kernel close to it.

For kernel (20), the Green's function is a 4×4 matrix diagonal in odd eigenfunctions. Therefore, the left-hand side of (23) is a product of the 2×2 determinant pertaining to the even eigenfunctions and the factors of the form λ_s — $G_{ss}(E;T)$ pertaining to the odd eigenfunctions. For $E < 0$, these factors cannot vanish, and therefore the energy spectrum of the relative motion of a pair is found from the vanishing condition for the determinant of form (23) constructed of the even eigenfunctions:

$$\lambda_1\lambda_2 - \lambda_1 G_{22} - \lambda_2 G_{11} + G_{11}G_{22} - G_{12}G_{21} = 0\,. \tag{25}$$

This condition allows both finding the discrete level of the bound state of the relative motion falling out of the continuum band and investigating specific features of the continuum.

Because one of the eigenvalues is negative ($\lambda_1 < 0$), Eqn (25) has a solution for $E < 0$. The character of the solution for a small coupling constant $w_0 = U_0 r_0^2$, which corresponds to the limit case $|E| \to 0$, can be analyzed by extracting the singular part of the integral (the Kantorovich technique) [57] determining the matrix element of the Green's function. The leading singularity has the form $G_{ss'} \sim -g \ln\left(\varepsilon_0/|E|\right)$, where ε_0 is the energy scale of the kinematically allowed region and g is the density of states (per spin) of the relative motion on the Fermi contour within this region. Such a singularity leads to the expression (the same as in the Cooper problem) for the binding energy

$$E_{\mathrm{b}} = \varepsilon_0 \exp\left(-\frac{1}{w_0 g}\right), \tag{26}$$

which is already nonzero for an arbitrarily small coupling constant if the density of states g of the relative motion is a finite quantity. This is the case for perfect mirror nesting of the Fermi contour that has a finite length within the kinematically allowed region. Otherwise, when the boundary separating the occupied and vacant states in the region Ξ consists of points, the density of states of the relative motion on the Fermi contour vanishes, $g = 0$, and the leading singularity of the matrix elements of the Green's function is weaker,

$$G_{ss'} \sim -g'|E| \ln\left(\frac{\varepsilon_0}{|E|}\right), \tag{27}$$

where g' is the derivative, with respect to energy, of the density of states of the relative motion calculated on the Fermi contour [56]. In the case of deviation from perfect mirror nesting, a bound state can arise if the effective coupling constant exceeds a certain threshold value.

Assuming the mirror nesting condition to be satisfied, we can represent the matrix elements of the Green's function in the weak coupling limit $w_0 g \ll 1$ as a sum of the singular, $G_{ss'}^{(\mathrm{s})}(E;T)$, and the energy-independent regular, $G_{ss'}^{(\mathrm{r})}(T)$, parts. In the weak-coupling limit, the regular contribution to $G_{ss'}$ can be neglected in determining the binding energy from Eqn (25).

7. Quasistationary pair states

For $E > 0$, Eqn (25) can allow complex-energy solutions: $E \to E - \mathrm{i}\Gamma/2$. The real part of the energy E then determines the position of the maximum density of pair states in the continuum band and Γ has the meaning of the QSS damping corresponding to this maximum. Separating the real and imaginary parts in (25) leads to a system of two equations for E and Γ. For perfect mirror nesting ($g \neq 0$), in the case of a QSS with small damping near the continuum band edge, the singular contribution to the matrix elements of the Green's function is estimated as $\mathrm{Re}\, G_{ss'}^{(\mathrm{s})} \sim g \ln(\rho/\varepsilon_0)$, where $\rho^2 = E^2 + \Gamma^2/4$, and the regular contribution (which must be taken into account in determining the QSS parameters) is independent of E and Γ. Evaluation of the imaginary part of the matrix element gives $\mathrm{Im}\, G_{ss'} \sim g \arctan(\Gamma/2E)$.

The graphical analysis of the system of equations for E and Γ shows [56] that QSSs may occur if the effective coupling constant exceeds a certain value $w_0^{(-)}$ dependent on the geometry of the kinematically allowed region and the form of the dispersion law. In the weak-coupling limit ($w_0 g \ll 1$), the QSS energy and damping are related as

$$\rho = \varepsilon_0 \exp\left(-\frac{1}{w_0^* g}\right), \qquad \arctan\left(\frac{2E}{\Gamma}\right) = C\,, \tag{28}$$

where $w_0^* \sim w_0$ and C are constants depending on the geometry of the region Ξ. Equation (21) for $g \neq 0$ can admit several solutions in the form of long-lived QSSs for a given $\mathbf{K}$. Different QSSs correspond to different $\mathbf{K}$.

The wave function of the relative motion of a pair, corresponding to both bound and quasistationary states, is a linear combination of two even eigenfunctions of kernel (20). One of these functions, belonging to the negative eigenvalue, is sign-alternating in the kinematically allowed region. As a consequence, the bound state and QSS under repulsion correspond to the wave function that in the momentum representation has a line of zeros intersecting the Fermi contour in the kinematically allowed region.

We emphasize that both the QSS and the bound state occur as solutions of the same equation (21) for the wave function of the relative motion of a pair.

The QSSs representing fluctuations in the superconducting order parameter exist in a limited temperature range, which is natural to associate [58] with the strong pseudogap region. The equation of motion of a pair (21) involves the particle interaction energy $U(\mathbf{k} - \mathbf{k}')$ with the weight $\Theta(\mathbf{k}';T)$, which singles out the kinematically allowed region at $T = 0$. The temperature weakening of the interaction between the components of a pair is caused by the temperature dependence of mean occupation numbers. The corresponding decrease in the effective coupling constant forbids the existence of a QSS with small damping at temperatures exceeding the characteristic temperature T_{str}^* related to the coupling constant value $w_0^{(-)}$. The temperature T_{str}^* assumes different (but close) values for a QSS with different momenta close to the momentum of superconducting condensate and has the same energy scale as T_{c}. The excess over T_{str}^* corresponds to the crossover from the state in which two-particle elementary excitations exist in the form of incoherent

pairs to a state with one-particle elementary excitations. Taking into account that pair incoherence occurs as T_c is exceeded, we can evaluate the crossover temperature as [56]

$$T^*_{\rm str} \approx T_c \left[\operatorname{artanh} \left(\frac{w_0^{(-)}}{w_0} \right) \right]^{-1} . \tag{29}$$

The effective coupling constant $w_0 = U_0 r_0^2$ shows the tendency to decrease with an increase in the doping level x caused by an increase in the screening of the Coulomb interaction. In underdoped compounds, the superconducting transition temperature $T_c(x)$ increases with x, and therefore the crossover temperature $T^*_{\rm str}(x)$ also first increases to its maximum, then begins decreasing, and can reach T_c for a certain x. Such $T^*_{\rm str}(x)$ behavior agrees qualitatively with the characteristic form of the upper boundary of a strong pseudogap (see Fig. 1).

8. Superconducting gap

Self-consistency equation (11) derived within the mean-field theory determines (under conditions of mirror nesting of the Fermi contour) the energy gap $|\Delta(\mathbf{k})|$ in the spectrum of one-particle superconductor excitations. In the case of pairing repulsion, the phase $\Phi(\mathbf{k})$ of the energy gap parameter $\Delta(\mathbf{k})$ must jump by π on a certain line of zeros of the parameter $\Delta(\mathbf{k})$ within the kinematically allowed region. It is only under this condition that the self-consistency equation can allow a nontrivial solution that has the same dependence on the momentum of relative motion as the kernel $U(\mathbf{k}-\mathbf{k}')$ whenever this kernel is degenerate. This resembles the situation with the EPI spectral density in the Eliashberg theory of superconductivity [59] which (by virtue of the dynamic restriction on the electron – phonon attraction) repeats, in fact, the energy dependence of the density of phonon states.

For symmetric kernel (20), the general solution of the self-consistency equation can be written as $\Delta(\mathbf{k}) = a - bk^2$, where a and b are determined by Eqn (11) [50]. In view of the dispersion law property $\xi(\mathbf{k}) = \xi(-\mathbf{k})$ and the symmetry of the kinematic restriction under the inversion transformation $\mathbf{k} \to -\mathbf{k}$, the odd eigenfunctions do not enter the expansion of the energy gap parameter in the complete system of functions $\varphi_s(\mathbf{k})$,

$$\Delta(\mathbf{k}) = \sum_{s=1}^{2} \Delta_s \, \varphi_s(\mathbf{k}) , \tag{30}$$

and this parameter is determined by two complex components Δ_1 and Δ_2 corresponding to the even eigenfunctions of (20). The energy gap parameter is conveniently represented as

$$\Delta(k) = b(k_0^2 - k^2) , \tag{31}$$

where b and $k_0^2 = a/b$ are determined by the system of equations [50]

$$\frac{w_0}{S} \sum_{\mathbf{k}} \frac{\Theta(\mathbf{k}; T) \, r_0^{2n} (k^{2n} - k_0^{2n})}{\sqrt{\xi^2(\mathbf{k}) + b(k_0^2 - k^2)^2}} = 2^{n+1} , \qquad n = 1, 2 , \tag{32}$$

into which the self-consistency equation with kernel (20) can be transformed.

In the weak-coupling limit, $b \to 0$ and the leading contribution to the integrals into which the sums in the system of equations (32) can be transformed is made by a small area of momentum space enveloping the part of the Fermi contour that pertains to the kinematically allowed region. The pair-excitation kinetic energy $2\xi(\mathbf{k})$ vanishes on the Fermi contour, and therefore, as $b \to 0$, the singular parts [which are proportional to $\ln(1/b)$] and the corresponding regular contributions [which are independent of b but, just as the coefficients at $\ln(1/b)$, depend on k_0^2] can be segregated from integrals (32). The system of equations thus transformed results in an exponential dependence of form (26) of the superconducting gap amplitude b on the coupling constant w_0 and determines the radius k_0 of the circle on which the gap vanishes.

This circle necessarily has an even (in view of the symmetry under the inversion transformation $\mathbf{k} \to -\mathbf{k}$) number of intersection points with the Fermi contour within the kinematically allowed region because otherwise the two equations of system (32) turn out to be inconsistent [50]. The circle of zeros $k = k_0$ crosses the Fermi circle when the latter is pronouncedly anisotropic. The approach of the Fermi contour to the circle of zeros can be regarded as an effective increase in the number of zeros, degenerating into a line when the Fermi contour becomes coincident with the circle $k = k_0$. This results in suppression of the energy gap amplitude even if the mirror nesting condition is satisfied [50]. Scattering processes taking the particle momenta outside the kinematically allowed region (e.g., scattering by impurities) violate the mirror nesting condition and eliminate the logarithmic singularity from the self-consistency equation.

The closeness of the Fermi level and the logarithmic Van Hove singularity of the density of states in an extended neighborhood of the saddle point of the electron dispersion law, encountered in cuprates [20, 60], and, accordingly, the hyperbolic metric of momentum space with a clearly pronounced effective-mass anisotropy [61] in the kinematically allowed region lead to isolines of the kinetic energy of the relative pair motion that almost coincide with the finite regions of the Fermi contour (approximate satisfaction of the mirror nesting condition) and promote an increase in the gap amplitude.

The superconducting phase transition temperature $T_{\rm sc}$ corresponding to the mean-field approximation can be found from the gap amplitude vanishing condition. This allows linearizing self-consistency equation (11), i.e., neglecting the term $|\Delta(\mathbf{k})|^2$ in the square root as $T \to T_{\rm sc}$. Using series expansion (30) of the energy gap parameter in eigenfunctions of kernel (20), which can be conveniently written as the spectral Hilbert – Schmidt expansion

$$U(\mathbf{k}-\mathbf{k}') = \sum_s \frac{\varphi_s(\mathbf{k}) \, \varphi_s^*(\mathbf{k}')}{\lambda_s} , \tag{33}$$

we can write the linearized self-consistency equation as

$$\sum_{s'=1}^{2} \left\{ \lambda_s \delta_{ss'} + \Lambda_{ss'}(T) \right\} \Delta_{s'} = 0 , \tag{34}$$

where

$$\Lambda_{ss'}(T) = \frac{1}{2} \sum_{\mathbf{k}} \frac{\varphi_s^*(\mathbf{k}) \, \varphi_{s'}(\mathbf{k}) \, \Theta(\mathbf{k}; T)}{|\xi(\mathbf{k})|} . \tag{35}$$

From the solvability condition for system of equations (34),

$$\det\left\{\lambda_s\delta_{ss'} + \Lambda_{ss'}(T)\right\} = 0\,, \tag{36}$$

we then find the temperature $T_{\rm sc}$.

The integrals to which the elements of matrix (35) are reduced depend both on the dispersion law of the relative motion of a pair and on the size and shape of the kinematically allowed region. To estimate these elements, we can use an approximate approach similar to the known method of zero-radius potential [32].

If we assume that in the limit as the efficiency of the screened Coulomb potential tends to zero, $r_0 \to 0$, the effective coupling constant $w_0 = U_0 r_0^2$ remains unchanged, then the two even eigenfunctions of kernel (20) prove to be piecewise constant [62],

$$\varphi_1(\mathbf{k}) = \pm\Xi^{-1/2}\left(\frac{\Xi_-}{\Xi_+}\right)^{\pm 1/2}, \qquad \varphi_2(\mathbf{k}) = \Xi^{-1/2}\,, \tag{37}$$

where Ξ is the area of the kinematically allowed region and Ξ_+ (Ξ_-) is the area of the part of this region in which the function $\varphi_1(\mathbf{k})$ corresponding to the negative eigenvalue $\lambda_1 < 0$ is positive (negative). The upper (lower) sign in (37) corresponds to $\mathbf{k} \in \Xi_+(\Xi_-)$.

The separation of the kinematically allowed region into the parts Ξ_+ and Ξ_- is determined by the kernel $U(\mathbf{k}-\mathbf{k}')$ of the operator of the pairing interaction in the equation for eigenvalues (18) irrespective of self-consistency equation (11) or equation (21) for the wave function of the relative motion of a pair.

Approximately representing the energy gap parameter $\Delta(\mathbf{k})$ by its values $\Delta_+ \equiv \Delta_1$ and $\Delta_- \equiv \Delta_2$ averaged over the respective regions Ξ_+ and Ξ_-, we can write Eqn (11) at $T = 0$ as the system of self-consistency equations

$$\begin{aligned} 2\Delta_1 &= -U_{11}f_1 - U_{12}f_2\Delta_2\,,\\ 2\Delta_2 &= -U_{21}f_1 - U_{22}f_2\Delta_2\,, \end{aligned} \tag{38}$$

where $f_s = \ln(2\varepsilon_s/|\Delta_s|)$ and $\varepsilon_1(\varepsilon_2)$ is the energy scale of the region Ξ_+ (Ξ_-).

Passing to the limit $r_0 \to 0$, we obtain a finite eigenvalue $\lambda_2 = (w_0\Xi)^{-1}$, while the other eigenvalue tends to infinity, $\lambda_1 \to -\infty$. As in the zero-radius potential method, we can make λ_1 a finite negative quantity by constructing, instead of (20), a new degenerate kernel on eigenfunctions (37) with the help of Hilbert–Schmidt expansion (33) and requiring that this new kernel lead to the same binding energy (26) of the pair as kernel (20) does [62]. As a result, we obtain $\lambda_1 = -\lambda_2$.

The new piecewise constant kernel is characterized by three parameters, U_{11}, U_{22}, and $U_{12} = U_{21}$, of which the first two pertain to the scattering inside the regions Ξ_+ and Ξ_-, and the third pertains to the scattering between these regions. For the parameters of the kernel, Suhl inequality (2) holds, and in the simplest case where $\Xi_+ = \Xi_-$, these parameters are given by [62]

$$U_{11} = U_{22} = 0\,, \qquad U_{12} = 2w_0\,. \tag{39}$$

The solution of the system of self-consistency equations (38) with kernel (39) leads to a piecewise constant energy-gap parameter

$$\begin{aligned} \Delta_+ &= 2\varepsilon_0\exp\left(-\frac{1}{w_0 g}\right), \qquad \mathbf{k}\in\Xi_+\,,\\ \Delta_- &= -\Delta_+\,, \qquad \mathbf{k}\in\Xi_-\,, \end{aligned} \tag{40}$$

where ε_0 is the energy scale of the kinematically allowed region corresponding to the total momentum $\mathbf{K}$ of the pair.

Matrix elements (35) become $\Lambda_{12} = 0$ and $\Lambda_{11} = \Lambda_{22} = (g/\Xi)\ln(2\gamma\varepsilon_0/\pi T)$, where $\ln\gamma \equiv C = 0.577$ is the Euler constant. The solution of Eqn (36) determining the superconducting transition temperature in the mean-field approximation gives the standard BCS relation between $T_{\rm sc}$ and the gap amplitude $\Delta \equiv |\Delta_\pm|$ at zero temperature: $2\Delta/T_{\rm sc} = 2\pi/\gamma \approx 3.52$.

In underdoped compounds, the critical temperature $T_{\rm c}$ increases from zero at x_* to its maximum value at $x_{\rm opt}$; after transition to the overdoped regime, it decreases to zero at x^*, which can be associated with the properties of the energy spectrum of cuprates and with the amplification of the Coulomb interaction screening with increasing x [47].

The vast region of the phase diagram above $T_{\rm c}(x)$ belongs to the pseudogap state in which both fluctuations of the superconducting order parameter [58] and the competition of the superconducting order with other ordered states inherent in cuprates can exist [6, 63]. Because $T_{\rm c} < T_{\rm sc}$, the relation $2\Delta/T_{\rm c} = 3.52(T_{\rm sc}/T_{\rm c})$ observed in underdoped cuprates [64] considerably exceeds the value 3.52 typical of the mean-field theory.

9. Fermi contour of doped cuprates

The superconducting state of a system of pairs with a large momentum can occur if the Fermi-contour mirror nesting condition is satisfied (at least approximately), i.e., if the electron dispersion law has a specific form providing a logarithmic singularity in the scattering amplitude.

The considerable on-site correlation energy allows considering the cuprate plane of the parent compound as a 2D Mott insulator [17] in which the energy band is split into two Hubbard subbands, of which the lower is occupied and the upper is vacant. In hole doping, a part of the electrons from the lower subband is removed the reservoirs, thus vacating the momentum space region bounded by the Fermi contour that originates in the neighborhood of the points $(\pm\pi/2, \pm\pi/2)$ in the form of small hole pockets with the area increasing in proportion to x.

At $T > T^*$, the data of angle-resolved photoemission spectroscopy (ARPES) point to the existence of a large Fermi contour with the area proportional to the electron concentration $(1-x)$ and the maximum spectral intensity [65, 66]. Weaker maxima form shadow bands caused by antiferromagnetic correlations [67]. The shadow bands are mirror reflections of regions of the main bands of the Fermi contour with respect to the boundaries of the magnetic Brillouin zone and, together with these regions, reproduce the hole pocket structure. The Fermi contour evolution upon doping is one of the key problems in cuprate physics.

The doping-induced evolution of a large Fermi contour (Fig. 4) can be described qualitatively within the rigid-band model [20] with the electron dispersion law

$$\varepsilon(\mathbf{k}) = -2t_1(\cos k_x + \cos k_y) + 4t_2\cos k_x\cos k_y\,, \tag{41}$$

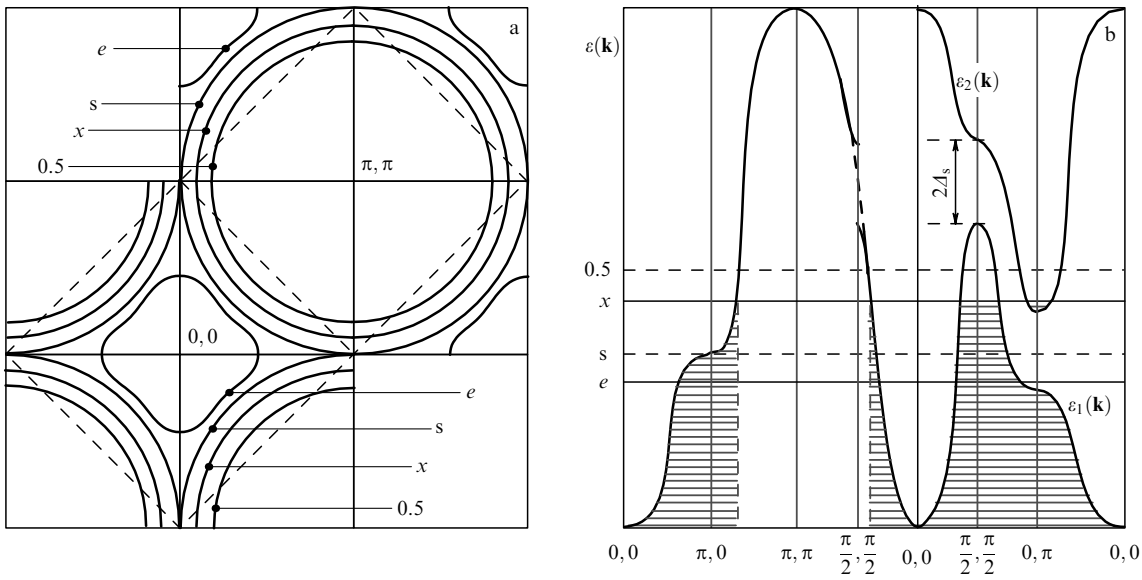

Figure 4. (a) Scheme of evolution of the electron (centered at the point 0, 0) and hole [centered at (π, π)] Fermi contour upon doping. The half-occupation isolines (0.5), the separatrix (s) passing through the saddle points $(\pm\pi, 0)$ and $(0, \pm\pi)$, and two isolines corresponding to the weak (x) and strong (e) hole doping are shown. The dashed lines indicate the boundary of the magnetic Brillouin zone. (b) The energy band structure for some directions in momentum space (schematically); regions of electron filling for weak doping are outlined. On the left: the energy spectrum corresponding to rigid-band model (41). On the right: two subbands (42) and the insulating forbidden band $2\Delta_s$ that occurs at the boundary of the magnetic Brillouin zone and is due to the short-range spin antiferromagnetic order.

where t_1 and t_2 are the electron hopping integrals between atoms of the first and second coordination spheres, respectively, and k_x and k_y are components of the momentum $\mathbf{k}$ in units $\bar{a}^{-1}$.

The hopping integrals are normally found in fitting the rigid-band model to the Fermi contour shape observed in ARPES experiments [68]. The parameters t_1 and t_2 are determined by the properties of not only the cuprate plane but also the reservoirs, and therefore the values of these parameters may be different in the families of cuprate compounds with different numbers of cuprate planes in an elementary cell. These parameters can be calculated (for each cuprate compound) within the density functional method [69, 70].

In the nearest-neighbor approximation ($t_2 = 0$) with half filling, the Fermi contour coincides with the boundary of the magnetic Brillouin zone, i.e., has the shape of a square with the nesting vector $\mathbf{Q} = (\pi, \pi)$; it passes through the saddle points $(\pm\pi, 0)$ and $(0, \pm\pi)$ and is a separatrix between two families of closed isolines. For $0 < t_2 < 2t_1$, the separatrix changes its shape but passes through the same saddle points and bounds the momentum-space region smaller than the half-filling region $x = 0$. Hence, the occupation $x = 0$ corresponds to the isolines with the energy higher than the saddle-point energy. The closed Fermi contour bounds the region of vacant states with the topological center (π, π). Doping brings the Fermi contour closer to the separatrix, and for a certain hole concentration $x = x_t$, the separatrix and the Fermi contour coincide. This corresponds to an umklapp of the topological center to the point $(0, 0)$ (for $x > x_t$, a closed line bounds the region of occupied electron states), i.e., to the electron topological transition [71] due to the Van Hove singularity at the saddle point.

The simply connected Fermi contour for holes of underdoped cuprates has the shape of a distorted square with rounded corners [20, 65, 66] aligned along the boundaries of the crystallographic Brillouin zone, inside which it bounds a momentum space region with the area proportional to the total hole concentration $(1 + x)$. In reduction to the first magnetic Brillouin zone, the arcs of the pockets of the Fermi contour are transferred into this zone. The shadow arcs remain in the second magnetic zone. The hole pocket area increases with x until a topological transition occurs at $x = x_t$, accompanied by sign reversal of the current charge carriers. The large Fermi contour bounding the electron occupation region with the area $(1 - x)$ assumes the shape of a distorted square oriented along the boundaries of the magnetic Brillouin zone.

The Fermi contour in the form of hole pockets satisfies perfect mirror nesting condition (14) at the momentum $\mathbf{K} = \mathbf{Q}$. The kinematically allowed region is a quarter of the crystallographic Brillouin zone containing a pocket.

Because of the antiferromagnetic spin correlations, an insulating gap Δ_s occurs at the boundary of the magnetic zone, which survives as a pseudogap in transition to the short-range order and decreases monotonically with increasing x up to the optimum doping [17]. The band with the dispersion law $\varepsilon(\mathbf{k})$ is split into two subbands with

$$\varepsilon_{1,2}(\mathbf{k}) = \varepsilon_+(\mathbf{k}, \mathbf{Q}) \pm \sqrt{\varepsilon_-^2(\mathbf{k}, \mathbf{Q}) + \Delta_s^2}\,, \tag{42}$$

where $2\varepsilon_\pm(\mathbf{k}, \mathbf{Q}) = \varepsilon(\mathbf{k}) \pm \varepsilon(\mathbf{k} + \mathbf{Q})$. The minus (plus) sign corresponds to the lower (upper) subband $\varepsilon_{1(2)}(\mathbf{k})$. Dispersion law (42) is defined in the magnetic Brillouin zone such that the Fermi contour can be obtained by simple extension to the crystallographic zone (Fig. 5). Because the insulating gap width Δ_s depends on x, the structure of the isolines $\varepsilon_{1,2}(\mathbf{k}) = \text{const}$ changes with doping [72], in contrast to the rigid-band model.

The pseudogap state of cuprates can be associated with the short-range order, which can explain the formation of

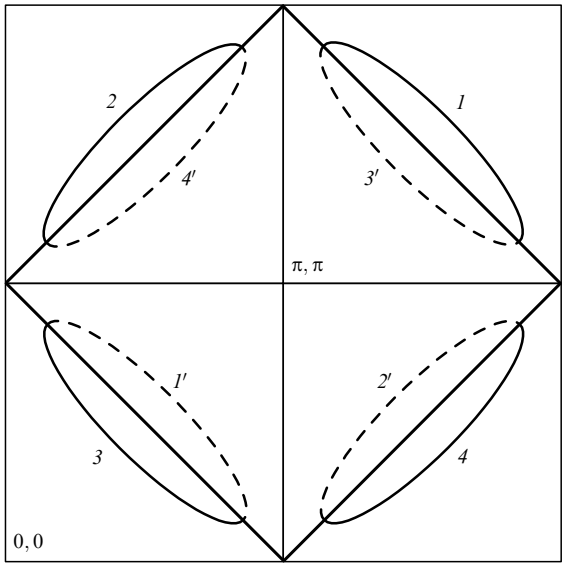

Figure 5. Fermi contour in the form of hole pockets in the neighborhood of $(\pi, 0)$-type points. Reduction to the magnetic Brillouin zone (the zone boundaries are marked out). The arcs of the Fermi contour arising in the scheme of extended zones are labeled with numerals (solid lines). Primed numbers label the Fermi-contour arcs with a low spectral intensity (dashed lines), occurring in the second magnetic Brillouin zone and corresponding to the shadow bands.

Fermi-contour arcs contracting to zero points of the superconducting gap parameter at T_c [73].

For weak doping, almost the whole first magnetic zone and comparatively small neighborhoods of $(\pi, 0)$-type points in the second magnetic zone correspond to the electron occupation. Accordingly, the first magnetic zone has small regions (pockets) with hole occupation. The excess holes introduced in these regions are the main current carriers in underdoped cuprates, and they alone participate in superconducting pairing, thus determining the particle number density $n_s \sim x$ in the condensate.

The occupation of the energy subbands is determined by the factors $\tilde{u}_{\mathbf{k}}$ and $\tilde{v}_{\mathbf{k}}$ in the Bogolyubov transformation diagonalizing the Hamiltonian that describes the electron–hole pairing responsible for the occurrence of a spin density wave (SDW). The occupation probability is characterized by the coefficient $\tilde{v}_{\mathbf{k}}^2$ which, in the order of magnitude, is equal to unity within the first magnetic zone. The spectral intensity of the ARPES signal is therefore high for the hole pocket arcs from the first magnetic zone. The substitution $\mathbf{k} \to \mathbf{k} + \mathbf{Q}$ corresponds to transition to the second magnetic zone. Because $\tilde{v}_{\mathbf{k}+\mathbf{Q}} = \tilde{u}_{\mathbf{k}}$, the ARPES response from the second magnetic zone, which keeps memory of the long-range antiferromagnetic order, is significantly weakened, which gives grounds for identification of these arcs with the shadow energy band [74].

The insulating s-wave forbidden band Δ_s, related to the SDW, occurs at the boundary of the magnetic Brillouin zone. Orbital antiferromagnetic (OAF) ordering in a cuprate plane with the order parameter, e.g., given by an orbital-current density wave with the d-wave symmetry (DDW) also leads to a pseudogap state [63]. In the region of relatively weak doping ($x \lesssim x_{\text{opt}}$), orbital and spin antiferromagnetism can coexist. This is promoted by the Fermi contour hole-pocket structure, which in the OAF pairing channel exhibits perfect nesting with the different pockets related by the same vector $\mathbf{Q} = (\pi, \pi)$ as in the SDW channel, leading to the doubling of an elementary cell [72]. The spectral intensities of the ARPES signal are determined by x-dependent coherence factors in the SDW and AOF channels of insulating pairing. The intensity redistribution between these two channels, observed as x increases, shows up as attenuation of the ARPES signal pertaining to the spin ordering with its simultaneous amplification in the OAF channel [75]. The energy band formation on the Fermi contour due to OAF ordering causes the chemical potential to be positioned inside this gap, and in this sense, the system in the pseudogap state behaves as an insulator.

The observation of resistance to an alternating current, due to the vortex motion in relatively weak (~ 1 T) magnetic fields in an optimally doped compound $YBa_2Cu_3O_{6+x}$ [76], suggests the conclusion [76] that the state occurring in the vortex core is insulating rather than metallic, as it would be in conventional superconductors. Such a conclusion, which agrees with the interpretation [63] of the weak pseudogap as an insulating state with a long-range orbital antiferromagnetic order, can be considered an argument in favor of the fact that cuprate superconductivity (at least up to the optimal doping level [77]) is due to the competition not with the normal Fermi liquid but with the insulating state existing above T_c as an independent pseudogap phase.

10. Order parameter

For a nonzero pair momentum, several crystal-equivalent momenta $\mathbf{K}_j$ exist, each of which corresponds to its own kinematically allowed region Ξ_j, and therefore the order parameter describing the superconducting state of pairs with $\mathbf{K}_j \neq 0$ must account for the degeneracy associated with the cuprate plane symmetry [78].

The order parameter, which has the meaning of the wave function of a pair, can be written in the mixed representation as

$$\Psi(\mathbf{R}, \mathbf{k}) = \sum_j \gamma_j \exp(\mathrm{i}\mathbf{K}_j\mathbf{R})\, \Psi_j(\mathbf{k})\,, \tag{43}$$

where $\mathbf{R}$ is the center-of-mass radius vector, $\Psi_j(\mathbf{k}) \sim \Delta_j(\mathbf{k})$ has the meaning of the wave function of the relative motion of a pair with the total momentum $\mathbf{K}_j$, and $\Delta_j(\mathbf{k})$ is the energy gap parameter with the domain of definition Ξ_j; the choice of the coefficients γ_j normalized by the condition $\sum_j |\gamma_j|^2 = 1$ is determined by the one-dimensional irreducible representation of the symmetry group of the cuprate plane, to which function (43) corresponds.

To determine the irreducible representation specifying the order parameter in (43), we must take the interelectron interactions into account, which, along with Coulomb repulsion (20), occur in the cuprate compound: the pairing attraction of electrons associated with the phonon exchange and strongly anisotropic pairing repulsion in the exchange of antiferromagnetic (AF) magnons. Considering these interactions to be small (compared to Coulomb repulsion) perturbations, we can find the explicit form of the γ_j.

The attraction associated with EPI, which is significant in the thin layer enveloping the Fermi contour and has the energy width $\sim \hbar\omega_D$, is characterized by a dimensionless coupling constant of the same order of magnitude as the

Coulomb coupling constant: $w_{\rm ph} \sim w_{\rm C}$ [37]. The ratio of the momentum-space areas in which the electron scattering due to the EPI attraction and Coulomb repulsion is significant has the order of magnitude $\hbar\omega_{\rm D}/\varepsilon_0 \ll 1$. This gives grounds to regarding the EPI-induced isotropic interaction as a small perturbation of repulsive potential (20).

The repulsive interaction associated with the exchange of antiferromagnetic magnons [38, 39] is essentially anisotropic and can approximately be represented as $U_{\rm AF}(\mathbf{k}) \sim U_0\chi(\mathbf{k})$, where U_0 is the Coulomb energy of the on-site correlation that defines potential (20) and $\chi(\mathbf{k})$ is the magnetic susceptibility. The interaction $U_{\rm AF}(\mathbf{k})$ is defined in the entire Brillouin zone and corresponds to electron attraction on neighboring sites. Hence, the pairing potential $U_{\rm AF}(\mathbf{k})$ leads to the d-wave order parameter [79]. Such an interaction can also be considered a small perturbation of Coulomb potential (20) because the magnetic susceptibility averaged over the Brillouin zone is $\bar{\chi} \ll 1$.

If the EPI attraction is predominant among the two perturbing interactions (which is certainly the case with overdoped cuprates), the coefficients γ_j in (43) define the irreducible representation $\mathrm{A}_{1\rm g}$: $\gamma_1 = \gamma_2 = \gamma_3 = \gamma_4$. Because the order parameter does not change sign under rotation by $\pi/2$ in the momentum space, the zeros of the order parameter are determined exclusively by the Coulomb repulsion, which corresponds to an extended s-wave symmetry. The irreducible representation $\mathrm{B}_{1\rm g}$: $\gamma_1 = -\gamma_2 = \gamma_3 = -\gamma_4$ can correspond to the dominating repulsion $U_{\rm AF}(\mathbf{k})$, which may occur in underdoped cuprates. In this case, the order parameter does change sign under rotation by $\pi/2$ in the momentum space, and the zeros due to the Coulomb repulsion are supplemented with four more zeros, which leads to an extended d-wave symmetry.

The order parameter normalization

$$\sum_{\mathbf{k}\in\Xi} \left|\Psi(\mathbf{R},\mathbf{k})\right|^2 = \frac{n_{\rm s}}{2}\,, \tag{44}$$

where $n_{\rm s}$ is the particle number density in the superconducting condensate determined by the carrier concentration in the conduction band and Ξ is the union of all regions Ξ_j when they do not overlap (or when their overlap can be ignored), results in the normalization of each of the functions $\Psi_j(\mathbf{k})$ to $n_{\rm s}/2$.

The system of eigenfunctions $\varphi_{js}(\mathbf{k})$ of the kernel $U(\mathbf{k}-\mathbf{k}')$ must be defined in each domain Ξ_j, and $\Psi_j(\mathbf{k})$ can be expanded in these functions:

$$\Psi_j(\mathbf{k}) = \sum_s \Psi_s\,\varphi_{js}(\mathbf{k})\,. \tag{45}$$

It is taken into account here that in view of the crystal equivalence of the regions Ξ_j, the expansion coefficients Ψ_s are independent of j, and the eigenfunctions $\varphi_{js}(\mathbf{k})$ for different j differ by the domain of definition only. The eigenfunctions of the kernel of the pairing interaction operator, defined in the entire kinematically allowed region,

$$\varphi_s(\mathbf{R},\mathbf{k}) = \sum_j \gamma_j \exp\left(\mathrm{i}\mathbf{K}_j\mathbf{R}\right)\varphi_{js}(\mathbf{k})\,, \tag{46}$$

form a complete orthonormal system of functions transforming under one of the one-dimensional irreducible representations of the point symmetry group of the cuprate plane.

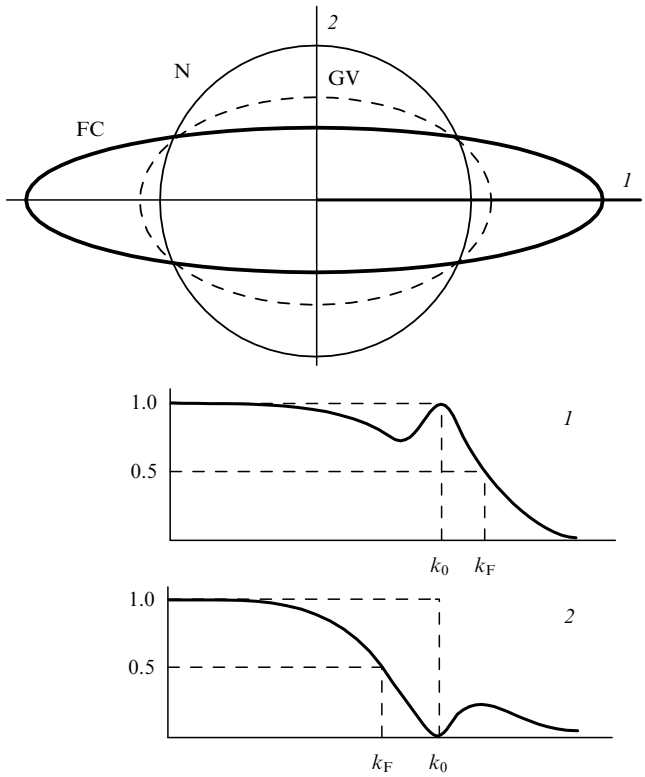

Figure 6. Top: the Fermi contour (FC, thick line), the line of order parameter zeros (circle N, thin solid line), and the line of group velocity zeros (GV, dashed line). Bottom: the dependence of the coherence factor $v_{\mathbf{k}}^2$ on the momentum of the relative motion of a pair for the directions denoted by numbers *1*, *2* in the top figure. Positions of the Fermi momentum $k_{\rm F}$ and the radius of the circle of order parameter zeros k_0 are indicated.

The expansion of the order parameter in the system of functions in (46) has the form

$$\Psi(\mathbf{R},\mathbf{k}) = \sum_s \Psi_s(\mathbf{R})\,\varphi_s(\mathbf{R},\mathbf{k})\,, \tag{47}$$

where the expansion coefficients (components of the order parameter) are written as

$$\Psi_s(\mathbf{R}) = \sum_{\mathbf{k}\in\Xi} \Psi(\mathbf{R},\mathbf{k})\,\varphi_s^*(\mathbf{R},\mathbf{k})\,. \tag{48}$$

We note that in the case of pairing repulsion, the order parameter has not less than two components [80].

The order parameter describing pairing of repulsive particles for a large pair momentum is related to three characteristic lines in the momentum space:

(1) A consequence of the mirror nesting is the separation of the occupied and vacant parts of the kinematically allowed region by finite regions of the Fermi contours, i.e., by the line on which the kinetic excitation energy of a pair of particles with momentum $\mathbf{K}$ vanishes, $2\xi(\mathbf{k}) = 0$, and the quasiparticle charge passes through zero.

(2) A consequence of the pairing repulsion is the line of zeros of the order parameter in the kinematically allowed region.

(3) The mirror nesting and pairing repulsion lead to the quasiparticle spectrum with an anisotropic energy gap and the group velocity vanishing within the kinematically allowed region on the line of minima of the quasiparticle excitation energy.

The Fermi contour, the line of zeros of the order parameters, and the line of minima of the quasiparticle excitation energy have common intersection points (Fig. 6). A consequence of the asymmetry between the occupied and vacant parts of the kinematically allowed region (and the corresponding asymmetry in the positions of maxima of the coherence factor $v_{\mathbf{k}}^2$, as shown in Fig. 6) is that in the superconducting transition, the chemical potential determined from the electroneutrality condition shows a shift $\Delta\mu \sim |\Psi|$ that is linear in the order parameter modulus [49].

11. Ginzburg – Landau functional

If the regions Ξ_j do not overlap, components (48) of the order parameter of a spatially homogeneous system are independent of the radius vector of the center of mass: $\Psi_s(\mathbf{R}) = \Psi_s$. In a spatially inhomogeneous system, the exponential factors (the wave functions of the free motion of the center of mass) in (43) are replaced by the wave functions of the center-of-mass motion in the external field. Hence, the use of the system of eigenfunctions (46) as a basis for the order parameter expansion makes its components (48) functions of $\mathbf{R}$.

The free energy of the system (per one cuprate plane) is a functional of the components $\Psi_s(\mathbf{R})$ of the order parameter,

$$F = \int f \, \mathrm{d}^2 R \,, \tag{49}$$

where f is the free energy density. Near the superconducting transition temperature, it can be represented as an expansion in powers of the components and their spatial derivatives,

$$f = f_0 + f_{\mathrm{g}} + f_{\mathrm{m}} \,, \tag{50}$$

where f_0 denotes contributions to the free energy density of the second and fourth order in $\Psi_s(\mathbf{R})$, f_{m} is the magnetic field energy density, and f_{g} is the gradient term in which it suffices to keep only the second-order contribution in $\nabla\Psi_s$ for slowly varying $\Psi_s(\mathbf{R})$.

The expansion of the free energy density in powers of the order parameter components $\Psi_s(\mathbf{R})$ can in general be written as [78]

$$f_0 = \sum_{ss'} A_{ss'} \Psi_s^* \Psi_{s'} + \frac{1}{2} \sum_{ss'tt'} B_{ss'tt'} \Psi_s^* \Psi_{s'}^* \Psi_t \Psi_{t'} \,. \tag{51}$$

In the case of kernel (20), only two order parameter components exist, and the summation indices in (51) and further on take the values 1 and 2. The matrices $A_{ss'}$ and $B_{ss'tt'}$ are functions of T and x and have three and five independent components, respectively.

The gradient term can be represented as [80]

$$f_{\mathrm{g}} = \frac{\hbar^2}{4m} \sum_{ss'} [\hat{\mathbf{D}} \Psi_s]^{\dagger} M_{ss'} [\hat{\mathbf{D}} \Psi_{s'}] \,, \tag{52}$$

where the positive definite matrix $M_{ss'}$ is a function of T and x and has three independent components. The operator of covariant differentiation with respect to coordinates of the center-of-mass radius vector is

$$\hat{\mathbf{D}} = -\mathrm{i}\nabla - \frac{2e}{\hbar c} \mathbf{A} \,, \tag{53}$$

where $\mathbf{A} = \mathbf{A}(\mathbf{R})$ is the vector potential determining the induction of the magnetic field averaged over the relative motion of the pair, $\mathbf{B} = \mathrm{rot}\,\mathbf{A}$. The field $\mathbf{A}$ includes the contributions of both the external magnetic field and the field that can be related to the appearance of spontaneous orbital currents.

The change in the energy density of the medium upon the occurrence of the magnetic field is written as

$$f_{\mathrm{m}} = \frac{z_0}{8\pi} (\mathrm{rot}\,\mathbf{A})^2 \,, \tag{54}$$

where z_0 is the distance between neighboring cuprate planes.

In compounds with several cuprate planes in an elementary cell, the concentration of holes introduced during doping is different in different planes and is determined from the condition of the electrostatic energy minimum [81]. The superconducting transition temperature T_{c} shows a universal dependence on the number n of cuprate planes in an elementary cell and reaches its maximum at $n = 3$ [82, 83]. This dependence can be explained [84] by the competition of the superconducting and insulating (pseudogap) ordered states described by different components Ψ_s of the order parameter.

The free energy is invariant under a unitary transformation of the order parameter components, realized by 2×2 matrices belonging to the SU(2) group. A special choice of such a transformation allows diagonalizing the matrices $A_{ss'}$ and $M_{ss'}$. Assuming that such a diagonalization has been performed, we can assume that $A_{ss'} = A_s \delta_{ss'}$ and $M_{ss'} = M_s \delta_{ss'}$, where A_s and M_s are functions of T and x.

The superconducting phase transition temperature $T_{\mathrm{sc}}(x)$ corresponding to the mean-field approximation is determined from the condition $\det A_{ss'}(T, x) = 0$, which, after diagonalization of the matrix $A_{ss'}$, assumes the form $A_1(T, x)\, A_2(T, x) = 0$. Because both components of the order parameter vanish at the same temperature, it is necessary that the two conditions $A_1(T, x) = 0$ and $A_2(T, x) = 0$ hold simultaneously; this is the case with repulsive-interaction pairing.

We note that states with a mixed symmetry of the $\mathrm{d}_{x^2-y^2} + \exp(\mathrm{i}\theta)\,\chi$ type, where χ is the contribution of states, e.g., with the s or d-symmetry and θ is the relative phase of the order parameter components, in general correspond to different mean-field temperatures of the phase transitions to states with the $\mathrm{d}_{x^2-y^2}$- and χ-symmetry (in particular, the phase transition can be absent altogether for one of such states) [85, 86].

Thus, near the phase transition line, we can set $A_s(T, x) = -\tau_1 A_s^{(0)}(x)$, where $A_s^{(0)}(x)$ are positive functions of doping,

$$\tau_1 = \frac{T_{\mathrm{sc}} - T}{T_{\mathrm{sc}}} \,,$$

and assume $|\tau_1| \ll 1$. The matrices $B_{ss'tt'}$ and $M_{ss'}$ do not vanish at $T = T_{\mathrm{sc}}$, and therefore, near the phase transition line, we can replace their argument T by T_{sc} and consider these matrices to be functions of x only. We note that such an approximation suffices when the transition temperature $T_{\mathrm{c}}(x)$ coincides with $T_{\mathrm{sc}}(x)$, which in cuprates is customarily believed to take place in overdoped regions only.

12. System of Ginzburg – Landau equations

The variational procedure leads to the system of two equations specifying the order parameter [80]

$$\frac{\hbar^2}{4m}\sum_{s'} M_{ss'}\left(-\mathrm{i}\nabla-\frac{2e}{\hbar c}\,\mathbf{A}\right)^2 \Psi_{s'} + \sum_{s'} A_{ss'}\Psi_{s'} + \sum_{s'tt'} B_{ss'tt'}\Psi_{s'}^*\Psi_t\Psi_{t'} = 0\,, \tag{55}$$

and the equation for the current density specifying the vector potential

$$\mathbf{j} = \sum_{ss'} M_{ss'}\left[\frac{\hbar e}{2\mathrm{i}m}\left(\Psi_s^*\nabla\Psi_{s'} - \Psi_{s'}\nabla\Psi_s^*\right) - \frac{2e^2}{mc}\,\Psi_s^*\Psi_{s'}\mathbf{A}\right], \tag{56}$$

where we use the notation

$$\mathbf{j} = z_0\,\frac{c}{4\pi}\,\mathrm{rot}\,\mathrm{rot}\,\mathbf{A}\,. \tag{57}$$

The system of boundary conditions can in particular be written as

$$\sum_{s'} M_{ss'}\left(\mathrm{i}\nabla+\frac{2e}{\hbar c}\,\mathbf{A}\right)\Psi_{s'}\mathbf{n} = 0\,, \tag{58}$$

where $\mathbf{n}$ is the outer normal to the boundary of a 2D region in the cuprate plane.

A system of two equations instead of a single equation for a system with a one-component order parameter can lead to several (for example, differing in the relative phase of components) nontrivial solutions corresponding to the minima of functional (49), their positions and energy values being dependent on the relation between the elements of the matrices $A_{ss'}$ and $B_{ss'tt'}$.

Gradient contribution (52) to the free energy describes the long-wave fluctuations of the order parameter with respect to the thermal equilibrium value. Order parameter (43) allows a special current state whose nature can be clarified using the Ginzburg – Landau equations [80]. Singling out the order-parameter phase

$$\Psi_s(\mathbf{R}) = \left|\Psi_s(\mathbf{R})\right| \exp\left[\mathrm{i}\Phi(\mathbf{R})\right], \tag{59}$$

we can write the superconducting current in the absence of the external magnetic field as

$$\mathbf{j} = \frac{\hbar e}{m}\,\overline{M}\,\nabla\Phi\,, \tag{60}$$

where

$$\overline{M} = \sum_{ss'} \Psi_s^* M_{ss'}\Psi_{s'}\,. \tag{61}$$

The components Ψ_s are rapidly varying functions of $\mathbf{R}$, and therefore the circulation of the current along any closed contour L_0 in the cuprate plane,

$$V = \oint_{L_0} \mathbf{j}\,\mathrm{d}\mathbf{l} = \frac{\hbar e}{m}\int_{S_0} \mathrm{d}^2R\,\mathbf{n}_3[\nabla\overline{M}\times\nabla\Phi]\,, \tag{62}$$

is generally nonzero; here, $\mathbf{n}_3$ is a unit vector of the normal to the plane and S_0 is the area of the surface bounded by the contour L_0. If the characteristic dimension of the contour L_0 considerably exceeds the scale $\sim K^{-1}$ on which the order parameter varies, then $V \approx 0$. The structure of the order parameter of the FFLO periodic structure type [87] corresponds to the division of the real 2D space into cells with the area $\sim K^{-1}$ such that the projection of the vector product in the $\mathbf{n}_3$ direction has opposite signs in the neighboring cells. Thus, as a result of long-wave fluctuations of the order-parameter phase (especially significant in underdoped cuprates because of the low phase stiffness), an antiferromagnetically ordered structure occurs (on the phase fluctuation scale) in the form of orbital current fluctuations.

We can estimate phase stiffness near the superconducting transition temperature. In the absence of a magnetic field, the gradient contribution to functional (49) can be written as

$$F_{\mathrm{g}}^{(2)} \simeq \frac{1}{2}\int \mathrm{d}^2R\,\rho_{\mathrm{s}}\,(\nabla\Phi)^2\,, \tag{63}$$

which implies that $\rho_{\mathrm{s}} = \hbar^2\overline{M}/2m$, where the order parameter components in $\overline{M}$ should be set equal to their equilibrium values. We thus have $\rho_{\mathrm{s}} \sim \tau_1$ near the transition temperature. If we assume that ρ_{s} depends linearly on temperature [88, 89], then owing to the order-parameter normalization in (44), the phase stiffness at zero temperature $\rho_{\mathrm{s}}(0)$ is proportional to the area of the kinematically allowed region $\Xi_j \sim x$. We note that the smallness of the phase stiffness for $x \to 0$ is not directly related to the x-dependence of the energy-gap parameter $\Delta(\mathbf{k})$.

The existence of a system of two equations instead of a single Ginzburg – Landau equation corresponding to the BCS model can result, as in the case of $s-d$ pairing [85], in several (e.g., differing in the relative phase) nontrivial solutions corresponding to Ginzburg – Landau functional minima with positions and energies dependent on the relation between the elements of the matrices $A_{ss'}$ and $B_{ss'tt'}$. Furthermore, a system of consistent equations for the order-parameter components can cause topological defects in the order-parameter phase, other than the vortices and antivortices that arise as solutions of the Ginzburg – Landau equations corresponding to the BCS model. This is the case, for example, with the coupling via the electromagnetic field only [90].

13. Spatially homogeneous order

In the absence of an external magnetic field and structural inhomogeneities, the superconducting state of a long-range order system is determined from the minimum condition for the free energy density f_0. The complex components of the order parameter can be specified in terms of their moduli ψ_1 and ψ_2 and the relative phase β:

$$\Psi_1 \equiv \psi_1 \exp(\mathrm{i}\Phi)\,, \qquad \Psi_2 \equiv \psi_2 \exp(\mathrm{i}\beta)\,\exp(\mathrm{i}\Phi)\,. \tag{64}$$

The obvious trivial solution $\psi_1 = \psi_2 = 0$ with an undefined relative phase corresponds to the free energy minimum at $T > T_{\mathrm{sc}}$. At $T < T_{\mathrm{sc}}$, nontrivial solutions exist for which the equilibrium values of the three parameters ψ_1, ψ_2, and β are determined by the x-dependent matrices $A_{ss'}$ and $B_{ss'tt'}$ [78].

The moduli of the order parameter components are related by normalization condition (44), $\psi_1^2 + \psi_2^2 = n_{\mathrm{s}}/2$, and therefore minimization of the free energy is reduced to a variational problem with two unknown quantities. Without

loss of generality, we can set $\psi_1 = \psi_2 \equiv \psi$ and write the free energy density as

$$f_0 = a_1\psi^2 + \frac{1}{2}\left(B + 2C\cos\beta + D\cos^2\beta\right)\psi^4\,, \tag{65}$$

where $a_1 \equiv -a\tau_1$, $a \equiv A_1^{(0)} + A_2^{(0)}$, and the other coefficients are expressed in terms of the elements of the matrix $B_{ss'tt'}$.

The search for the extremum of function (65) shows that at $T < T_{\rm sc}$, the minimum is attained for $\beta = \pi$ and $\psi \neq 0$ under the condition $C \geqslant D$. Otherwise, a nontrivial solution corresponds to the relative phase $\beta \leqslant \pi$ defined by the relation $\cos\beta = -C/D$.

The equality $C(x) = D(x)$ can be regarded as an equation describing the doping level x_0 for which the superconducting order changes qualitatively. In a small neighborhood of the point x_0, the ratio $C/D \equiv c(x)$ can be represented as $c(x) = 1 + c'(x_0)(x - x_0)$. If we assume that the state with the relative phase $\beta = \pi$ corresponds to the doping $x > x_0$ ($c'(x_0) > 0$), then for $x < x_0$, the relative phase is $\beta(x) < \pi$ with $\beta(x)$ being a continuous function of its argument such that $\beta(x) \to \pi$ as $x \to x_0$.

The order parameter that distinguishes between the two thermal equilibrium superconducting phases with $\beta < \pi$ (β phase) and $\beta = \pi$ (π phase) can naturally be defined as $\alpha = \pi - \beta$, and therefore $\alpha = 0$ for $x > x_0$ and $\alpha > 0$ for $x < x_0$. Near the transition point x_0 and for $\tau_1 \ll 1$, the free energy density can be written as an expansion in even powers of α and ψ.

The free energy minimum is attained at $\alpha = 0$ in the π phase ($x > x_0$) and at $\alpha^2 = 2c'(x_0)(x_0 - x)$ in the β phase ($x < x_0$). In a small neighborhood of the phase transition point x_0, the squared modulus of the equilibrium order parameter is equal to $\psi^2 = a\tau_1/(B - D)$, and hence the expression for the free energy density of the β phase becomes

$$f_\beta = f_\pi - v\tau_1^2(x - x_0)^2\,, \tag{66}$$

where $f_\pi = -a\tau_1\psi^2 + (B - D)\psi^4/2$ is the free energy density of the π phase and $v = a^2D/(B - D)^2 > 0$.

14. Spontaneous orbital currents

Different signs of the real components of the order parameter (which corresponds to the relative phase equal to π) necessarily occur in superconducting pairing with repulsive interaction [78]. A deviation in the relative phase from π corresponds to the solution of the self-consistency equation with complex coherence factors and allows a rather demonstrative interpretation. The phase change of the annihilation operator of an electron with the spin $\sigma = \uparrow, \downarrow$ at the crystal lattice site with a radius vector $\mathbf{n}$ can be related to the vector potential $\mathbf{A}(\mathbf{n})$ of the magnetic field as

$$\hat{c}_{\mathbf{n}\sigma} \to \hat{c}_{\mathbf{n}\sigma}\exp\left[\mathrm{i}\,\frac{e}{\hbar c}\,\mathbf{A}(\mathbf{n})\mathbf{n}\right]. \tag{67}$$

Then, the phase $\beta(\mathbf{n}, \mathbf{n}')$ of the anomalous average $\langle\hat{c}_{\mathbf{n}\uparrow}\hat{c}_{\mathbf{n}'\downarrow}\rangle$ (which determines the superconducting order parameter), written in the site representation is given by

$$\beta(\mathbf{n}, \mathbf{n}') = \pi - \frac{e}{\hbar c}\left[\mathbf{A}(\mathbf{n})\mathbf{n} + \mathbf{A}(\mathbf{n}')\mathbf{n}'\right]. \tag{68}$$

Expressing $\mathbf{n}$ and $\mathbf{n}'$ in terms of the radius vectors of the center of mass, $\mathbf{R} = (\mathbf{n} + \mathbf{n}')/2$, and of the relative motion of a pair, $\mathbf{r} = \mathbf{n} - \mathbf{n}'$, we can segregate the contribution to the superconducting condensate phase that depends on $\mathbf{R}$ only,

$$\Phi_{\rm c}(\mathbf{R}) = \frac{2e}{\hbar c}\,\mathbf{A}(\mathbf{R})\mathbf{R}\,,$$

of which the expansion of the free energy density is independent.

The correction to π [except for the phase $\Phi_{\rm c}(\mathbf{R})$ of the superconducting condensate] in (68) due to the relative motion determines the relative phase α of the order parameter components, which near the phase transition point $x = x_0$, where $\alpha \ll 1$, can be estimated as

$$\alpha \approx -\frac{e}{2\hbar c}\,\frac{\partial A_k}{\partial x_l}\,x_k\,x_l\,. \tag{69}$$

Here, we imply summation from 1 to 2 over the repeated indices labeling the 2D coordinates x_k of the radius vector $\mathbf{r}$ of the relative motion.

It can be assumed that the occurrence of a superconducting order parameter phase different from π is due to the orbital antiferromagnetic (OAF) ordering, which manifests itself in the superconducting state as antiferromagnetically correlated orbital current circulations [91] and can survive above $T_{\rm c}$ as a long-range [63] or short-range [92] OAF order. In this case, the real magnetic field in (69) generated by orbital currents can be treated as a certain gauge field that relates the charge and current degrees of freedom (ψ and α, respectively) and is similar to the gauge fields introduced into the Ginzburg–Landau functional, for instance, in the boson scheme of spin–charge separation [93, 94]. In neighboring crystal cells, the current circulations have opposite signs. In the Ginzburg–Landau phenomenology, the order parameter should be understood as being averaged over the relative motion of a pair, and therefore, recalling the checkered order in the distribution of orbital currents, we can estimate the root-mean-square (within a cell) value of the OAF-ordering parameter as

$$\alpha^2 \simeq \frac{\pi^2}{2}\left(\frac{e}{2\hbar c}\right)^2\frac{B^2}{K_j^2}\,, \tag{70}$$

where B is the magnetic induction of the orbital current field averaged over a cell.

The occurrence of orbital currents in the superconducting state requires taking the contribution $f_{\rm m}(\alpha) = \varkappa\alpha^2$ into account in the Ginzburg–Landau functional. This contribution is proportional to B^2 and is related to the energy of the magnetic field of the orbital currents. It can be verified that the inequality $\varkappa > 0$ forbids the occurrence of the minimum free energy density $f_0 + f_{\rm m}(\alpha)$ for $\alpha \neq 0$. This naturally makes it necessary to consider the competition between the superconducting and insulating OAF pairing channels [95]. We note that the breakdown of cuprate superconductivity by a magnetic field leads to precisely the insulating state [76, 77].

The OAF ordering considered in Ref. [63] as a pseudogap phase state (a flux phase in a two-dimensional lattice [96], the same as the toroidal magnetic ordering in three-dimensional crystals [97, 98]) reduces the cuprate-plane magnetic translational symmetry because of the occurrence of a d-wave symmetry, which corresponds to the orbital currents circulating along the chemical bonds between nearest-neighbor copper atoms. The state of orbital currents that does not violate the translational symmetry (but violates the time

reversal symmetry [99]) can be represented in the same way. In this case, the circular current corresponds to the orbital motion along the chemical bonds between the nearest-neighbor copper and oxygen atoms in each quarter of an elementary cell [99]. An experimental determination of the type of OAF order encounters great difficulties because the generated magnetic fields are weak [17]. In this connection, a lively discussion [102] concerning the existence and a possible origin of orbital antiferromagnetism in cuprates was stimulated by paper [100], reporting the observation of a spontaneous time-reversal symmetry breaking in ARPES experiments with circularly polarized light, and by communication [101] that reported on the magnetic order not violating the translational symmetry, observed in the experiment on elastic diffraction of polarized neutrons in the YBaCuO system.

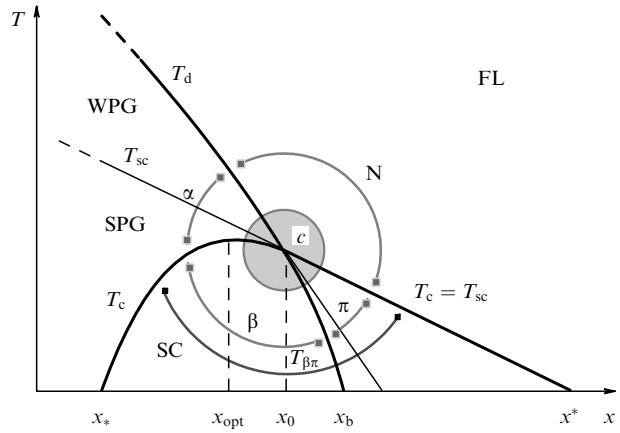

Figure 7. Region of the phase diagram corresponding to the coexistence of the insulating OAF and SC phases in the neighborhood of the tetracritical point c (encircled). Thick lines show phase transitions. The WPG region corresponds to a weak pseudogap with a long-range OAF order and the SPG region belongs to a strong pseudogap with developed superconducting order-parameter fluctuations against the background of the long-range OAF order. The superconducting (SC) region is separated into two phases: the conventional superconducting phase π and the phase β in which superconductivity coexists with antiferromagnetically ordered orbital circular currents. A region of developed OAF fluctuations against the background of long-range superconducting order lies between the β and π phases. FL is Fermi liquid.

15. Free energy

Spontaneous orbital currents can also occur in the absence of a superconducting order. The corresponding insulating OAF order in a 2D system is characterized by a single parameter that has the meaning of the magnetization difference in two sublattices of an orbital antiferromagnet. This difference is proportional to α, and therefore the free energy density (in the absence of superconductivity) near an OAF transition can be represented as an expansion in even powers of α,

$$f_{\mathrm{d}} = a_2\,\alpha^2 + \frac{1}{2}\,b_2\,\alpha^4\,, \tag{71}$$

where b_2 is a positive function of x and the coefficient $a_2(T, x)$ vanishes at the insulating phase transition temperature $T_{\mathrm{d}}(x)$ corresponding to the mean-field approximation; for $|\tau_2| \ll 1$, where $\tau_2 = (T_{\mathrm{d}} - T)/T_{\mathrm{d}}$, we can write $a_2 = -a'\tau_2$, where a' is a positive function of x. The energy $f_{\mathrm{m}}(\alpha)$ of the magnetic field of spontaneous currents, proportional to α^2, is included in the first term in (71) via a redefinition of the dielectric phase transition temperature $T_{\mathrm{d}}(x)$.

Consideration of the spatially homogeneous case in the absence of an external magnetic field allows establishing a relation between the two types of ordering. In this case, neither ψ nor α depend on the radius vector $\mathbf{R}$ of the center of mass, and the contribution of only the field of spontaneous orbital currents must be kept in the gradient term (52) of the Ginzburg – Landau functional. Because the vector potential of this field is $\mathbf{A} \sim \alpha$, it follows that the gradient term averaged over the relative motion of a pair can be written as $f_{12} = b_{12}\psi^2\alpha^2$, where b_{12} is an x-dependent phenomenological parameter.

In the case of pairing repulsion, self-consistency equation (11) determines the position of the line of zeros on which the energy gap parameter $\Delta(\mathbf{k})$ reverses sign and the phase $\Phi(\mathbf{k})$ of anomalous average (10) jumps by π. The phase $\Phi(\mathbf{k})$ itself is determined by Eqn (11) up to an arbitrary $\mathbf{k}$-independent summand α that manifests itself in the gradient term of the Ginzburg – Landau functional and is therefore related to the orbital current degree of freedom of the relative pair motion. Hence, the orbital current proportional to α plays the role of the order parameter. To derive the equation determining it, we must diagonalize the Hamiltonian in Eqns (5) and (6) using a Bogolyubov transformation that couples particles in the superconducting and insulating OAF pairing channels. For this reason, transformation (8), which only accounts for superconducting pairing, involves arbitrariness in the definition of the relative phase α and does not allow determining its $\mathbf{k}$-dependence. Correspondingly, in the phenomenological approach, the phase component α of the two-component superconducting order parameter should be treated as averaged (within a crystal elementary cell) over the relative pair motion.

The zeros of the modulus (ψ) and phase (α) of the superconducting order parameter do not coincide on the Fermi contour, which makes the system insensitive to scattering by nonmagnetic impurities.

Thus, the free energy density describing the competition between superconductivity and orbital antiferromagnetism assumes the form [78, 103]

$$f = a_1\psi^2 + a_2\alpha^2 + \frac{1}{2}\,b_1\psi^4 + b_{12}\,\psi^2\alpha^2 + \frac{1}{2}\,b_2\alpha^4 \tag{72}$$

up to fourth-order terms. The decomposition of free energy density (72) makes sense in a comparatively small region of the phase diagram in which the graphs of the dependences $T_{\mathrm{sc}}(x)$ and $T_{\mathrm{d}}(x)$ either intersect or pass close to each other.

It is natural to consider the corresponding phase transition temperatures $T_{\mathrm{d}}(x)$ and $T_{\mathrm{sc}}(x)$, which are determined in the mean-field approximation in the absence of coupling between competing ordered states, i.e., for $b_{12} = 0$ in (72), to be monotonically decreasing functions of x because doping causes suppression of both orbital antiferromagnetism and superconductivity. The properties of the phase diagram of cuprates (see Fig. 1) suggest the assumption that orbital antiferromagnetism dominates for small x but is suppressed faster than superconductivity as x increases. This enables the graphs of the functions $T_{\mathrm{d}}(x)$ and $T_{\mathrm{sc}}(x)$ to intersect at a certain point corresponding to x_0 (Fig. 7). The assumption that the superconducting transition temperature calculated in the mean-field approximation in the absence of orbital antiferromagnetism exceeds the temperature of the mean field of an orbital antiferromagnetic transition for a weak

doping in the absence of superconductivity ($T_{sc} > T_d$) is in contradiction with the phase diagram structure. The decomposition of the free energy density (72) is valid in a small neighborhood of the intersection point of the functions $T_d(x)$ and $T_{sc}(x)$, and therefore the extension (shown in Fig. 7) of the lines outside this neighborhood is rather dubious.

16. Tetracritical point

For $T > \max(T_d, T_{sc})$, the free energy minimum is reached at $\psi = 0$ and $\alpha = 0$, which corresponds to the normal (N) phase. For $x < x_0$, the boundary separating the normal and insulating α phase, in which $\psi = 0$ and $\alpha^2 = -a_2/b_2$, is the phase transition line $T = T_d(x)$. The lower boundary of the α phase is the line (defined by the condition $b_2 a_1 = b_{12} a_2$) of phase transition into the β phase,

$$T_{\alpha\beta} = T_{sc} T_d \frac{b_2 a - b_{12} a'}{b_2 a T_d - b_{12} a' T_{sc}}, \tag{73}$$

in which superconductivity coexists with orbital antiferromagnetism. In the β phase, both components of the order parameter are nonzero:

$$\psi^2 = -\frac{b_2 a_1 - b_{12} a_2}{b_1 b_2 - b_{12}^2}, \qquad \alpha^2 = -\frac{b_1 a_2 - b_{12} a_1}{b_1 b_2 - b_{12}^2}. \tag{74}$$

For $x > x_0$, the transition from the N phase to the superconducting π phase with the order parameter $\psi^2 = -a_1/b_1$, $\alpha = 0$ occurs at $T = T_{sc}(x)$. The temperature

$$T_{\beta\pi} = T_{sc} T_d \frac{b_1 a' - b_{12} a}{b_1 a' T_d - b_{12} a T_{sc}} \tag{75}$$

corresponds to the transition between two superconducting phases. The line $T = T_{\beta\pi}(x)$ starts at the intersection point of the lines $T = T_d(x)$ and $T = T_{sc}(x)$ for $x = x_0$ (point c in Fig. 7) and terminates on the x axis at a point $x_b > x_0$. Thus, the point c is a *tetracritical point*, at which four phase transition lines meet, and the point with the coordinates $x = x_b$ and $T = 0$ acquires the meaning of a *quantum critical point*.

The scheme of phase symmetry submission in the neighborhood of a tetracritical point is determined by the cuprate plane symmetry. In the case of a square lattice of the two-dimensional crystal class $G = C_{4v}$, the extended point group of the most symmetric N phase is the direct product

$$G_N = G \times R \times U(1),$$

where R denotes the group consisting of the identity transformation and the time reversal transformation R (reversing the directions of the currents) and U(1) is a gauge transformation group. The transition from the N phase to the superconducting π phase is accompanied by a gauge symmetry loss, and therefore the point symmetry group of the π phase is a nonmagnetic crystal class $G_\pi = G \times R$. In the transition from the N phase to the insulating α phase, some elements of the crystal symmetry (to which the H group, which is one of the index-2 subgroups of G, now corresponds) are lost because of the occurrence of spontaneous circular currents. The point symmetry group of the α phase is the superconducting magnetic class with the set of elements $G_\alpha = (H + RgH) \times U(1)$, where g is an element of the group G not belonging to H. As a result of the loss of gauge symmetry in the transition from the α phase to the β phase, the point symmetry group of the β phase is the magnetic class $G_\beta = (H + RgH)$. The group G_β is simultaneously one of the subgroups of G_α and G_π which are, in turn, subgroups of the group G_N. The group $G = C_{4v}$ has two subgroups of index 2: $H = C_4$ and $H = C_{2v}$. The former leads to the ferromagnetic class $C_{4v}(C_4)$ and the latter corresponds to the antiferromagnetic class $C_{4v}(C_{2v})$ with the distribution of currents in a 2D flux phase [78].

17. Phase portrait

In the sector of the phase diagram corresponding to the normal phase, the free energy has a minimum at $\psi = 0$, $\alpha = 0$, which in passage through the line $T = T_d(x)$ to the α phase shifts along the α axis to the point $\psi = 0$, $\alpha = \sqrt{-a_2/b_2}$. However, this minimum is the only singular point of free energy not in the entire existence region of the insulating α phase but only in its upper part with $T_{sc}(x) < T < T_d(x)$. Passing through the line $T = T_{sc}(x)$ to the minimum determining the thermal stable insulating state adds a saddle point at $\psi = \sqrt{-a_1/b_1}$, $\alpha = 0$. In the β phase for $T < T_{\alpha\beta}$, the orbital antiferromagnetism and superconductivity coexist. The free energy density has an absolute minimum at $\alpha \neq 0$ and $\psi \neq 0$ and two saddle points (on both coordinate axes). On the line $T = T_{\beta\pi}$ of the transition from the β phase to the π phase, the minimum on the ψ axis shifts and replaces one of the saddle points. In passing through the line $T = T_d(x)$, the saddle point on the α-axis shifts to the origin (Fig. 8).

In the neighborhood of the tetracritical point, the states from the sector $T_{sc}(x) < T < T_d(x)$ corresponding to the absolute minimum and to the saddle point have close free energies. Therefore, the probability of the fluctuation-induced incoherent long-lived quasistationary states of superconducting pairs with the relative phase π (to which the state of the saddle point $\psi = \sqrt{-a_1/b_1}$, $\alpha = 0$ corresponds) is sufficiently high in the temperature range $T_c(x) < T < T_{sc}(x)$. The decay of such a quasistationary state (QSS), followed by a decrease in the modulus of the SC order parameter ψ from $\psi = \sqrt{-a_1/b_1}$ to zero with increasing the relative phase α from zero to the equilibrium value $\alpha = \sqrt{-a_2/b_2}$, can be regarded as the creation of decoupled pairs of oppositely oriented circular currents or unbound vortex–antivortex pairs. The intermediate states during the QSS decay are the fluctuation states of the β phase belonging to close isolines passing from the neighborhood of the saddle point to the neighborhood of the free-energy absolute minimum.

Thus, for $x < x_0$, the temperature $T_{sc}(x)$ that is the upper bound of the region of developed fluctuations of the SC order parameter modulus is not associated with any phase transition. It can be considered as the upper bound of the phase diagram region in which vortex orbital currents exist owing to the creation and decay of QSS superconducting pairs with the relative phase π. Such currents can lead to a substantial increase in the Nernst effect observed in cuprates in the strong-pseudogap region. Therefore, the temperature $T_{sc}(x)$ for $x < x_0$ can be identified with the crossover that bounds this region from above: $T_{sc}(x) \approx T^*_{str}(x)$. We note that a strong pseudogap can penetrate the extremely low-doping region, $x < x_*$, in which $T_c(x) = 0$.

In passage through the line $T = T_{sc}(x)$ from the N phase to the π phase, the free-energy minimum shifts from the point $\psi = 0$, $\alpha = 0$ to the point $\psi = \sqrt{-a_1/b_1}$, $\alpha = 0$. This mini-

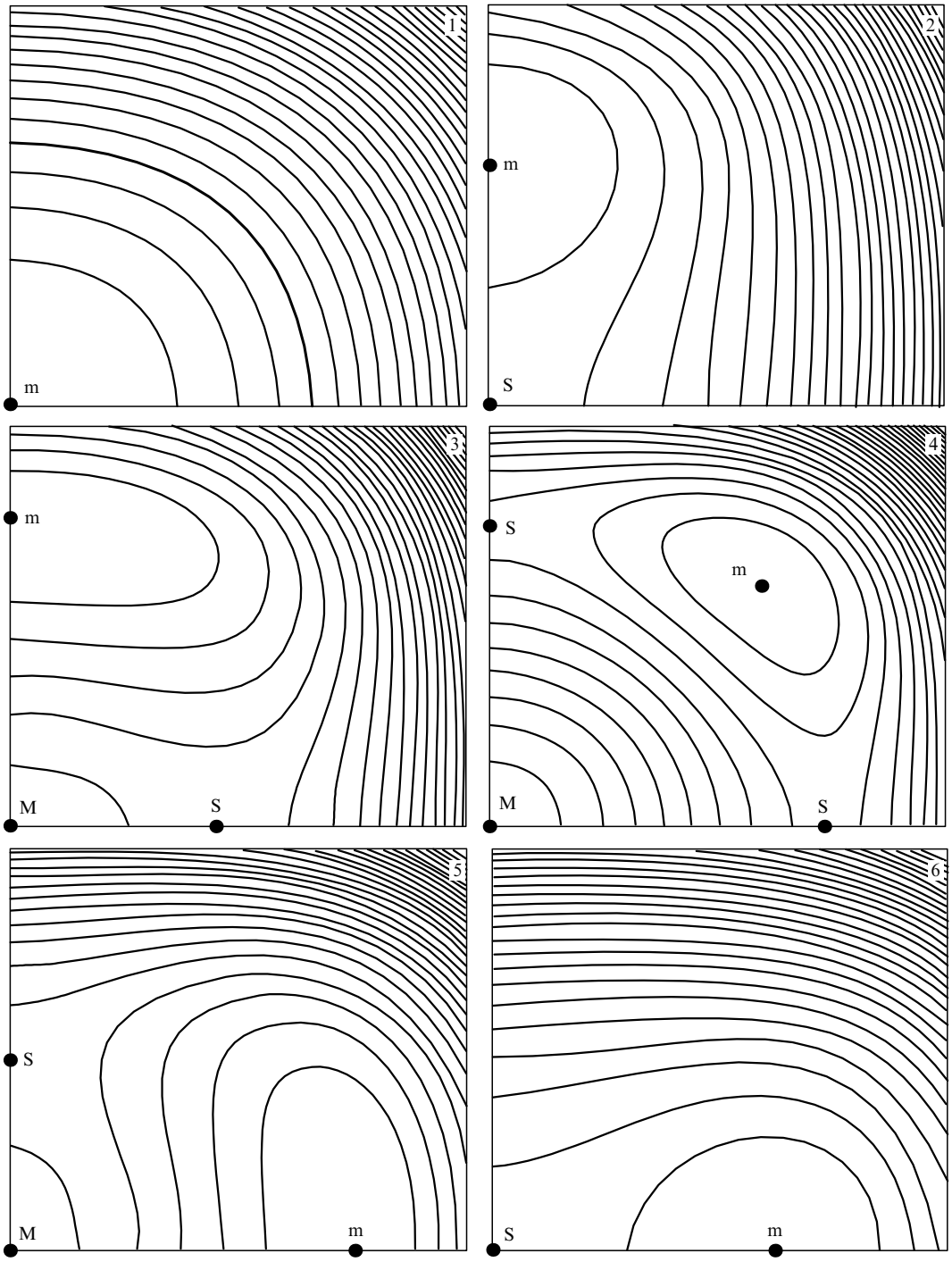

Figure 8. Topology of free energy isolines in coordinates ψ (horizontal axis) and α (vertical axis). Numbers denote sectors of the phase diagram near the tetracritical point: normal Fermi-liquid (1), weak pseudogap (2), strong pseudogap (3), superconducting β phase (4), region of developed OAF fluctuations against the background of long-range superconducting order (5), and superconducting π phase (6). The maxima (M), minima (m), and saddle points (S) are marked with filled dots.

mum is absolute in the entire region of the π phase existence, but a saddle point with coordinates $\psi = 0$, $\alpha = \sqrt{-a_2/b_2}$ appears in the sector $T_{\beta\pi}(x) < T < T_{\mathrm{d}}(x)$ (see Fig. 8). In the neighborhood of the tetracritical point c, the free energies at the minimum and at the saddle point are close, and therefore the fluctuation-generated QSS orbital circular currents are highly probable in the sector $T_{\beta\pi}(x) < T < T_{\mathrm{d}}(x)$. The decay of such a QSS, i.e., a decrease in the relative phase of the order parameter from its saddle-point value $\alpha = \sqrt{-a_2/b_2}$ to zero with a simultaneous increase in the modulus of the order parameter ψ from zero to the thermal equilibrium value $\psi = \sqrt{-a_1/b_1}$, proceeds through nonequilibrium states of the β phase. For $x_0 < x < x^*$, the temperature $T_{\mathrm{sc}}(x)$ corresponding to the mean-field approximation is the temperature of the phase transition from the N to the π phase, $T_{\mathrm{sc}}(x) = T_{\mathrm{c}}(x)$.

The two-component order parameter, naturally following from the concept of large-momentum repulsion-induced

pairing accounts for the charge and current degrees of freedom and necessarily leads to the picture of developed order-parameter fluctuations. The phase transition between the normal and superconducting π phase in the overdoped region of the phase diagram proceeds for $\alpha = 0$ and can be described within the Landau theory of phase transitions with a single-component order parameter.

The concentration $x_{\rm opt}$ formally determined by the position of the $T_{\rm c}(x)$ maximum is certainly lower than the concentration of the tetracritical point, $x_{\rm opt} < x_0$, and therefore, when extended to the low-temperature range, the lower bound of the π phase ends at a point $x_{\rm b}$ in the interval (x_0, x^*). In this interval, the temperature lowering after the phase transition $\mathrm{N} \to \pi$ first brings the system to the region of developed fluctuations in the form of QSS orbital circular currents and then the system undergoes a second phase transition between two superconducting states at a temperature $T_{\beta\pi}(x)$. Such a phase transition within the superconducting state could be registered, for instance, by the anomaly in the temperature dependence of heat capacity. The modulus of the order parameter ψ remains continuous at the phase transition temperature $T_{\beta\pi}(x)$, and the relative phase α, which is equal to zero in the π phase, becomes nonzero at $T < T_{\beta\pi}(x)$ [78].

18. Diamagnetism of the pseudogap state

The observation [26, 104, 105] of the giant Nernst effect in an extended part of the pseudogap region in hole-doped cuprates can be thought of as evidence of the existence of vortex-type excitations at temperatures much higher than $T_{\rm c}$.

The Nernst effect (the thermogalvanomagnetic effect, i.e., the appearance of an electric field perpendicular to mutually perpendicular magnetic field and temperature gradient) is rather weak in normal metals in which transport phenomena are associated with quasiparticle excitations and transfer. The Nernst effect is considerably amplified in the transition of a metal into the state of a type-II superconductor in the region between the first and second critical magnetic fields. In this case, a vortex excited in a magnetic field $\mathbf{B}$ drifts in the temperature gradient field with the velocity $\mathbf{v} \sim \nabla T$, leading to the Nernst electric field $\mathbf{E} = [\mathbf{B} \times \mathbf{v}]/c$. We can assume that developed fluctuations in the phase of the superconducting order parameter occur in the strong pseudogap region, violating the phase coherence [58].

The elementary vortex excitations leading to the phase coherence loss occur in a system with strong electron correlations within various theoretical schemes. In the boson version [93, 94] of the charge and spin separation scheme [106], the phase coherence violation at $T_{\rm c}$ is associated with the thermal excitation of spins in the form of free spinon vortices in a rather wide temperature range with the upper boundary having the interpretation of the holon condensation temperature and corresponding to depairing of incoherent superconducting pairs.

The low phase stiffness leads to developed fluctuations suppressing the long-range order in a 2D system, and therefore $T_{\rm c}$ can be regarded as the temperature of the Berezinski–Kosterlitz–Thouless transition corresponding to the occurrence of unbound vortices and antivortices of the superconducting order parameter phase. The Dirac character of the nodal quasiparticle spectrum [16] allows the description (using the analogy with quantum electrodynamics in two dimensions) of the pseudogap state within the framework of the phenomenological scheme [107] in which vortices and antivortices (which are elementary excitations in this scheme) manifest themselves as topological defects of the order parameter phase and are due to quantum or thermal fluctuations. Such defects can result from sign reversal of separate current circulations [108] in a flux phase.

A consequence of the superconducting pairing with large momentum and screened Coulomb repulsion is the occurrence of a QSS having momenta close to the superconducting condensate momentum and existing as incoherent pair states in a sufficiently wide temperature range above $T_{\rm c}$. The upper boundary of this range can be associated with the crossover between states of the strong and weak pseudogap. The dependence of the crossover temperature on doping in (29) agrees qualitatively with the upper boundary of the region in which a giant Nernst effect is observed [26, 104, 105].

The thermodynamic states in the region of a strong pseudogap, corresponding to the absolute minimum at $\psi = 0$, $\alpha = \sqrt{-a_2/b_2}$ and to the saddle point at $\psi = \sqrt{-a_1/b_1}$, $\alpha = 0$, have close free energies. Therefore, the probability of the fluctuation-induced long-lived QSS of superconducting pairs with the relative phase π (to which the saddle-point state corresponds) is rather high in the temperature range $T_{\rm c}(x) < T < T_{\rm sc}(x)$. The decay of such a QSS, followed by a decrease in the modulus of the superconducting order parameter from $\psi = \sqrt{-a_1/b_1}$ to zero, with the relative phase increase from zero to the thermal equilibrium value $\alpha = \sqrt{-a_2/b_2}$, can be regarded as the creation of pairs of oppositely oriented circular currents. The intermediate states during QSS decay are fluctuation β-phase states that belong to the isolines connecting the neighborhoods of the saddle point and the free-energy absolute minimum.

The temperature $T_{\rm sc}(x)$ for $x < x_0$ bounding the region of developed fluctuations of the superconducting order parameter modulus from above is not related to any phase transition and can be considered the upper boundary of the region in the phase diagram where orbital vortex currents exist owing to the occurrence and decay of the QSS of superconducting pairs with the relative phase π. Such currents can be responsible for a notable amplification of the Nernst effect, and therefore $T_{\rm sc}(x)$ for $x < x_0$ can be identified with the crossover bounding the strong-pseudogap region from above. In the neighborhood of the tetracritical point, $T_{\rm sc}(x) \approx T^*_{\rm str}(x)$. We note that the strong pseudogap can penetrate the region of an extremely weak doping $x < x_*$.

In the absence of phase coherence above $T_{\rm c}$, the circular orbital currents can lead to the giant diamagnetism (nonlinear Meissner effect), which was predicted in [78, 103] and observed in underdoped cuprates in the temperature range above $T_{\rm c}$ [25].

The order parameter defined as

$$\alpha^2 = -\frac{a_2 + dB^2}{b_2} \tag{76}$$

corresponds to the homogeneous state of the α phase in a magnetic field. The magnetic susceptibility of the α phase can accordingly be represented as

$$\chi_\alpha \approx \chi_{\rm N} + \frac{2\,\tilde{d}\,b_2}{a_2}\,, \tag{77}$$

where $\chi_{\rm N}$ is the magnetic susceptibility of the N phase, $\tilde{d} = d_1 + d_2$ in the case of a transverse field and $\tilde{d} = d_1$ in the

case of a longitudinal field relative to the cuprate plane. Here, d_1 and d_2 are phenomenological parameters in the expansion of the free energy of the Landau antiferromagnet in power series of the order parameter and magnetic field strength [109]. In the neighborhood of the tetracritical point, a transition from the paramagnetic N phase to the diamagnetic state of the α phase occurs at the temperature

$$\tilde{T}_{\mathrm{d}} = T_{\mathrm{d}}\left(1 - \frac{b_2\chi_{\mathrm{N}}}{2\tilde{d}a'}\right). \tag{78}$$

19. Cuprate electrodynamics

The electromagnetic response of superconducting cuprates differs essentially from that of conventional superconductors [23]. In contrast to conventional superconductors, cuprates do not have a clearly pronounced superconducting gap in the frequency dependence of the real part $\sigma_1(\omega, T)$ of the complex conductivity. The residual absorption in the superconducting state persists down to extremely low frequencies in all the superconducting cuprate compounds and is satisfactorily described by the two-fluid Drude model [23]. The conductivity $\sigma_1(\omega, T)$ for $T < T_{\mathrm{c}}$ turns out to be suppressed in a wide energy range (compared to the conductivity observed for $T \gtrsim T_{\mathrm{c}}$). The conductivity passes through the minimum and shows the Drude behavior $\sigma_1 \sim \omega^{-2}$ as $\omega \to 0$. The minimum of $\sigma_1(\omega, T)$ is not related to T_{c} and frequently occurs in the normal state above T_{c} (Fig. 9).

The integral characteristic of the electromagnetic response is the total spectral weight

$$S = \int_0^{\infty} \sigma_1(\omega, T)\,\mathrm{d}\omega \sim \frac{\pi n e^2}{2m^*}, \tag{79}$$

where m^* has the meaning of the effective carrier mass and the total particle number density $n = n_{\mathrm{n}} + n_{\mathrm{s}}$ is the sum of the particle number densities of the normal (n_{n}) and superconducting (n_{s}) components. Only a rather small part of the spectral weight from the low-frequency spectral region can pertain to the superconducting condensate occurring at $T < T_{\mathrm{c}}$: the coherent (Drude) component of the spectral weight exceeds the spectral weight of the condensate.

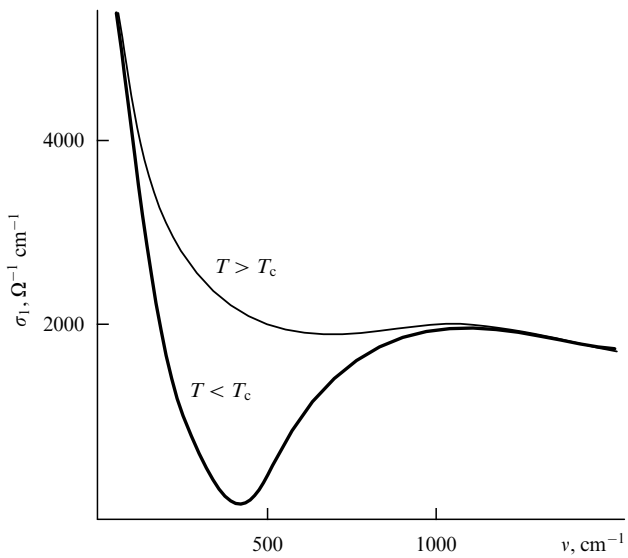

Figure 9. Frequency dependence (schematically, according to [23]) of the real part σ_1 of the complex conductivity at $T < T_{\mathrm{c}}$ (thick line) and $T > T_{\mathrm{c}}$ (thin line).

Attempts to explain the residual conductivity by the d-wave symmetry of the superconducting gap have led to a quantitative contradiction with experimental data in that the conductivity in the low-frequency range turns out to be too high [23]. A finite density of states in the superconducting gap region is the necessary condition for the appearance of residual conductivity. Because of the order parameter zeros, the quasiparticles are excited even at very low temperatures. But in a pure d-wave superconductor, we have $\sigma_1(\omega, T) \to 0$ as $\omega \to 0$ for $T \ll T_{\mathrm{c}}$.

It is assumed [23] that the observed large value of the residual low-temperature conductivity can be due to the inhomogeneities inherent in the cuprate electron system.

The residual optical conductivity and the related large density of the particles outside the condensate at $T < T_{\mathrm{c}}$ naturally follow from the Coulomb mechanism of pairing with large momentum. First, when the mirror nesting condition holds on only a part of the Fermi contour, the other part of it corresponds to gapless excitations responsible for the increase in the normal component n_{n} of the carrier number density and, therefore, for the increase in the Drude component of the complex conductivity. Second, if, as is the case with cuprates for a relatively low doping level, the Fermi contour has the form of small hole pockets and the mirror nesting holds on the entire Fermi contour, then different spectral intensities correspond to parts of each pocket belonging to different magnetic Brillouin zones. The pair creation probability is then determined by the spectral intensity of the pocket part belonging to the second (shadow) magnetic zone. This results in a relatively low particle number density $n_{\mathrm{s}} \sim \tilde{u}_k\tilde{v}_k$ of the superfluid component (compared to the particle number density $n_{\mathrm{n}} \sim \tilde{u}_k^2 - \tilde{v}_k^2$ of the normal component) and in a relative increase in the Drude component of conductivity. Here, $\tilde{u}_k$ and $\tilde{v}_k$ are coherence factors in the Bogolyubov transformation that describe the electron – hole pairing accompanied by an SDW. We note that the difference $\tilde{u}_k^2 - \tilde{v}_k^2$ specifying the Drude component of the optical conductivity is quite analogous to the difference between the electron and hole concentrations $n_{\mathrm{e}} - n_{\mathrm{h}}$ (due to doping) that characterizes the semimetal – insulator transition [110, 111] and the difference $n_{\uparrow} - n_{\downarrow}$ of spin populations in the case of superconducting pairing in a weak ferromagnet [112, 113]. Moreover, a large number of closely located order-parameter zeros occurring in pairing repulsion leads to a high (compared with a d-wave superconductor) density of states inside the energy gap and to a large number of quasiparticles excited at $T < T_{\mathrm{c}}$.

The optical sum rule [114 – 116] allows analyzing the spectral weight redistribution upon the occurrence of a superconducting condensate. In conventional superconductors, such a redistribution occurs in the frequency range $0 < \hbar\omega \lesssim 2\Delta$, where 2Δ is the superconducting energy gap.

The spectroscopic measurements [117] show that the spectral weight of a superconducting condensate in cuprates is related not only to the states $\hbar\omega \lesssim 2\Delta$ in the energy gap region but also, and to a large extent, to the spectral weight transfer from much more energetic states. This apparent violation of the optical sum rule finds a qualitative explanation in the assumption that the superconducting condensation energy in cuprates is associated not with the lowering of the potential energy, as is the case with pairing attraction in a

narrow (of the order of $\hbar\omega_D$) energy band, but with the lowering of the kinetic energy of carriers [118, 119], which is possible in paring repulsion in a much wider energy range $\varepsilon_0 \gg \hbar\omega_D$.

Segregating the contributions of kinetic and potential energies to the superconducting order parameter is rather arbitrary and generally makes no sense in the absence of pairing interaction. However, the occurrence of the order parameters (linear in the absolute value) of the chemical potential shift [49] leading to a redistribution of carriers over momenta within the kinematically allowed region formally allows relating the superconducting condensation energy to the lowering of the kinetic energy of carriers participating in the pairing.

The suppression of antiferromagnetic correlations and the occurrence of superconductivity with increasing doping are accompanied by an increase in the superfluid density $\rho_s = 4\pi n_s e^2/m^* \sim x$, which is correlated with the superconducting transition temperature: $\rho_s \sim T_c$ [120]. Refining this Uemura graph gives the relation $\rho_s \sim \sigma_{dc} T_c$ [121], which is satisfied in a wide doping range for all the investigated cuprate compounds. Here, σ_{dc} is the normal-state conductivity in a constant field. The correlation dependence $T_c \sim n_s/m^*$ does not appear in the BCS theory, but occurs for the Bose – Einstein condensation [122].

20. Cuprate spectroscopy

The experimental data obtained by the photoemission and tunnel spectroscopy methods definitely point to a substantial distinction between the spectra of cuprates and conventional superconductors. The ARPES measurements of photoemission intensity proportional to the probability of detection of an electron with given energy E and momentum $\mathbf{p}$ show that for a fixed $\mathbf{p}$ [in the $(\pi, 0)$ direction of the energy gap maximum], the broad quasiparticle maximum observed in the normal state of overdoped cuprates is very rapidly transformed (near T_c) into a narrow peak in passing to the superconducting state. The leading edge of this peak has an energy shift equal to the energy gap and the trailing edge smoothly passes into a notable dip in the spectral density followed by a sufficiently broad maximum, which at higher energies tends to the value corresponding to the normal state. Such a 'peak – dip – hump' (PDH) structure (Fig. 10) of the photoemission spectrum at $T < T_c$ reflects the features of superconducting pairing in cuprates.

In underdoped cuprates, the PDH structure of the ARPES spectrum also takes place at $T < T_c$, but the structure is rapidly smoothed above T_c and, moreover, the position of the leading edge of the quasiparticle peak is preserved. This implies that a superconductor does not go to the normal Fermi-liquid state at T_c and can be treated as evidence of the fact that incoherent pairs remain in the pseudogap (insulating) state at $T > T_c$.

Such a PDH structure is also observed in tunnel spectra, which, in addition, show asymmetry under sign reversal of the bias voltage. This electron – hole asymmetry can naturally be explained [49] as the asymmetry between the occupied and vacant parts of the kinematically allowed region, with the relation between its areas determining the shift of the chemical potential with a component linear in $|\Delta(\mathbf{k})|$ (the necessity of introducing such a component for the explanation of the asymmetry of cuprate tunnel spectra is pointed out in Ref. [123]).

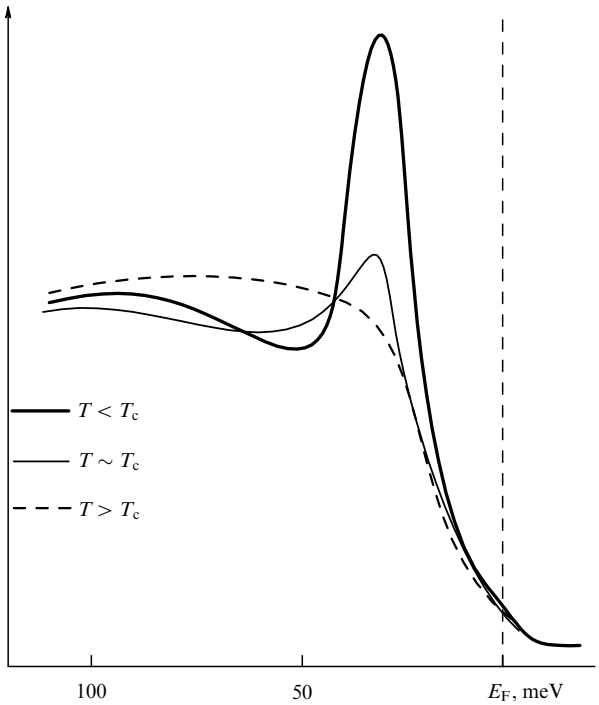

Figure 10. Structure of the ARPES spectrum, typical of cuprates, for a $(\pi, 0)$ type direction in the superconducting $(T < T_c)$ state immediately above the phase transition temperature $(T \gtrsim T_c)$ and in the normal state $(T > T_c)$.

It is natural to assume that the PDH structures of the photoemission and tunnel spectra have a common origin.

The differential conductivity (tunnel conductance) $\sigma_t = dI/dV$, where I is the current through the tunnel contact and V is the bias voltage, can be written as

$$\sigma_t = -A \int d^2k \left[u_{\mathbf{k}}^2 \, \delta(E_{\mathbf{k}} - eV) + v_{\mathbf{k}}^2 \, \delta(E_{\mathbf{k}} + eV) \right], \qquad (80)$$

where A is a positive constant, $E_{\mathbf{k}}$ is quasiparticle energy (14), and $u_{\mathbf{k}}^2$ and $v_{\mathbf{k}}^2$ are coherence factors that are defined in (9) and have the form

$$u_{\mathbf{k}}^2 = \frac{1}{2}\left(1 + \frac{\xi_{\mathbf{k}}}{E_{\mathbf{k}}}\right), \qquad v_{\mathbf{k}}^2 = \frac{1}{2}\left(1 - \frac{\xi_{\mathbf{k}}}{E_{\mathbf{k}}}\right), \qquad (81)$$

where $2\xi_{\mathbf{k}}$ is the kinetic energy of a pair, Eqn (4). The conductance is defined by the first summand in (80) for a positive bias $(eV > 0)$ and by the second summand for a negative bias $(eV < 0)$.

If the line of minima of the quasiparticle excitation energy $E_{\mathbf{k}}$ coincides with the Fermi contour (which is the case not only with an isotropic s-wave gap, but also with a d-wave gap for which the lines of zeros are straight lines $k_y = \pm k_x$), the conductance in (80) has an obvious symmetry under the bias sign reversal: $\sigma_t(-V) = \sigma_t(V)$. The assumption [123, 124] that the superconducting gap depends on the kinetic energy of the relative motion of the pair, $\Delta_{\mathbf{k}} = \Delta(\xi_{\mathbf{k}})$, leads to an asymmetric conductance because different values of the coherence factors $u_{\mathbf{k}}^2$ and $v_{\mathbf{k}}^2$ correspond to bias values equal in modulus but opposite in sign. The superconducting gap considered in [124], with the energy slope $\Delta(\xi) = a - b\xi$, where a and b are phenomenological parameters, corresponds to the fact that the line of minima of the quasiparticle

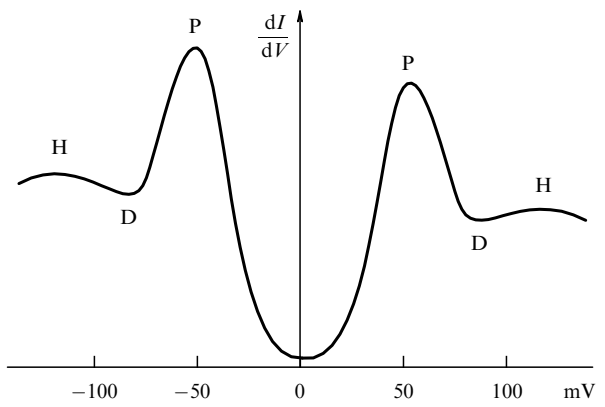

Figure 11. A characteristic asymmetric tunnel spectrum of a cuprate compound at $T < T_c$ showing the PHD structure.

energy $E_{\mathbf{k}}$ lies entirely either inside or outside the Fermi contour and therefore has no intersection points with the Fermi contour (except at the nodal points if, for instance, the gap has a d-wave symmetry and the parameters a and b depend on the angular variable ϑ in the momentum space).

In the large-momentum pairing with Coulomb repulsion, the quasiparticle energy also has the line of minima noncoincident with the Fermi contour, but the line of gap zeros crosses the Fermi contour, which is responsible for the specific behavior of the coherence factors (see Fig. 6).

In sectors corresponding to $k_F(\vartheta) < k_0$ [where $k_F(\vartheta)$ is the Fermi momentum dependent on the angular variable], the factor $v_{\mathbf{k}}^2$ vanishes for k_0, showing its minimum in the neighborhood of this point. In sectors $k_F(\vartheta) > k_0$, the factor $v_{\mathbf{k}}^2$ has a maximum at the point k_0 where $v_{\mathbf{k_0}}^2 = 1$. For a hole-pocket type Fermi contour, the energy corresponding to the maximum exceeds (on the average) the energy of the minimum, and therefore the minimum and maximum at k_0 in the integration in (80), which smoothes these extremums [52], manifest themselves as a shallow dip followed by a small hump of the conductance (Fig. 11).

21. Andreev reflection

An electron moving towards the interface between a normal metal (N) and a superconductor (S) can experience Andreev reflection [125], forming a hole with sign reversal of the energy (counted from the chemical potential) and of all the three velocity components. For conventional superconductors at $T < T_c$, a consequence of the Andreev reflection is a twofold increase in the NS transition conductivity for voltages below the superconducting gap, compared to the conductivity at $T \gtrsim T_c$. In superconducting cuprates, the NS interface conductivity is much lower [126]. This experimental fact can be explained by the assumption that cuprate superconductivity is due to Coulomb pairing with large pair momenta, leading to a change in the Andreev reflection kinematics [127].

In underdoped cuprates, the Fermi contour with perfect mirror nesting is represented by four hole pockets centered at the points $(\pm\pi/2,\ \pm\pi/2)$. For each of the four crystal-equivalent pair momenta $\mathbf{K}_j = (\pm\pi, \pm\pi)$, the nonintersecting kinematically allowed regions are the corresponding quarters of the Brillouin zone (Fig. 12).

Because the line of zeros of the quasiparticle group velocity and the Fermi contour (the line of zeros of the quasiparticle charge) do not coincide in each kinematically

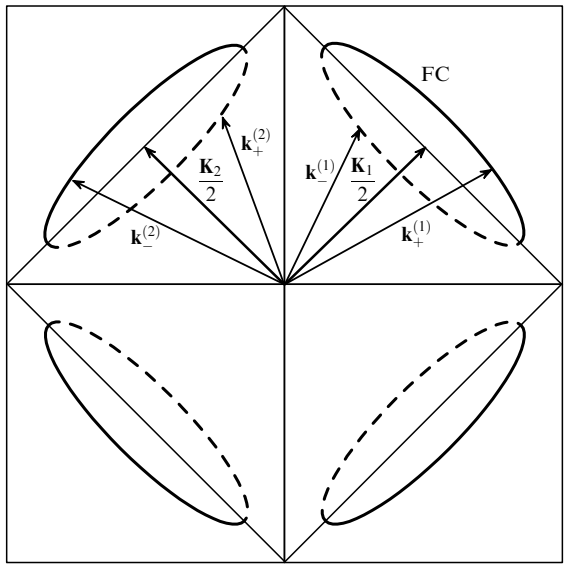

Figure 12. Pairs with large momenta $\mathbf{K}_j = (\pm\pi, \pm\pi)$. The direction of the momentum $\mathbf{K}_1$ coincides with the normal to the NS interface. The particle with the momentum $\mathbf{k}_+^{(2)}$ undergoes Andreev reflection with the momentum $\mathbf{k}_-^{(2)}$, and the particle with the momentum $\mathbf{k}_+^{(1)}$ penetrates into the superconductor as a hole with the momentum $\mathbf{k}_-^{(1)}$ (geometrical Andreev transmission).

allowed region Ξ_j (except at their intersection points, see Fig. 6), a range of directions exists in the momentum space where reflection does not entail sign reversal of the quasiparticle charge, and therefore only a part of the electrons with momenta not belonging to this range undergo Andreev reflection.

If the normal to the NS interface corresponds to the direction of one of the equivalent momenta $\mathbf{K}_j$ ($\mathbf{K}_1$ in Fig. 12), the direction of motion of a hole that appears after the Andreev reflection turns out to be not exactly opposite to the momentum $\mathbf{K}_1$. The angle of the Andreev reflection is determined by the total pair momentum. A particle approaching the NS interface with a momentum $\mathbf{k}_+^{(1)}$ finds a partner with the momentum $\mathbf{k}_-^{(1)}$ to make a pair in the region Ξ_1. In this case, the direction of motion of the newly formed hole corresponds to transmission (the geometrical Andreev transmission), and therefore the probability of Andreev reflection is equal to zero for the entire Ξ_1 region. The current transported by the newly formed pair with the momentum $\mathbf{K}_1$ is partially compensated by the current of the hole that occurred simultaneously, and, in contrast to the case $\mathbf{K} = 0$, the entire Ξ_1 region fails to contribute to the total Andreev reflection probability.

If a particle approaches the NS phase boundary with the momentum $\mathbf{k}_+^{(2)}$, it finds a partner with the momentum $\mathbf{k}_-^{(2)}$ in the Ξ_2 region (see Fig. 12) and the direction of the occurring hole corresponds to reflection.

In momentum space, two direction sectors exist such that the Fermi momentum k_F in one of them exceeds the momentum k_m for which the quasiparticle energy minimum is attained and the quasiparticle group velocity vanishes ($k_F > k_m$); in the other sector, on the contrary, $k_F < k_m$. Particle transmission from the N region into the superconductor is shown in Fig. 13 for the directions in the sector $k_F > k_m$.

Moving deep into the superconductor, a particle with an energy $E_1 < E_{min}$, where E_{min} is the minimum quasiparticle

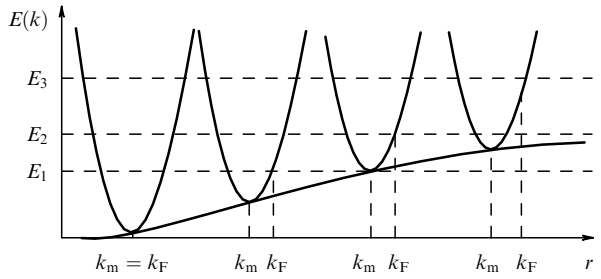

Figure 13. Electron transmission through the NS phase boundary: Andreev reflection (E_1), Andreev transmission due to charge asymmetry (E_2), and normal transmission (E_3).

energy in the depth of the superconductor, first reaches a point at which the particle momentum is k_F and the quasiparticle charge reverses sign. Then, the particle reaches the point of the quasiparticle energy minimum, where the velocity of the relative motion is reversed and the hole is reflected into the N region (Andreev reflection).

Moving towards the S region, a particle with an energy $E_2 < E_F$, where E_F is the Fermi energy in the depth of the superconductor, crosses the Fermi contour passing onto the hole branch of the spectrum (see Fig. 13). But it does not reach the turning point of the group velocity, and therefore the newly formed hole continues moving inside the superconductor (Andreev transmission due to charge asymmetry, as distinct from the barrier transmission [128] also occurring in conventional superconductors).

At an energy $E_3 > E_F$, the particle reaches neither the point k_F nor the point k_m, and therefore the ordinary quasiparticle transmission into the superconductor occurs (see Fig. 13).

In the other direction sector of the momentum space, $k_m > k_F$, the region of Andreev transmission due to charge asymmetry is absent because during the particle motion deep into the superconductor, the turning point of the relative motion velocity of the pair is reached before the point of quasiparticle charge reversal.

22. Competition of pairing interactions

The degeneration in crystal-equivalent pair momenta, which occurs in the case of large-momentum pairing with screened Coulomb repulsion, is removed by interactions due to phonon or antiferromagnetic magnon exchange; these processes determine the symmetry of the superconducting order parameter. Furthermore, these interactions (which may not be negligibly small compared to the Coulomb repulsion) contribute to the binding energy of the pair, thus influencing the superconducting transition temperature.

The competing pairing interactions can be taken into account in self-consistency equation (11) by replacing the true kernel $U(\mathbf{k}-\mathbf{k}')$ of the interaction operator by an approximate degenerate piecewise constant kernel leading to the same binding energy of the pair as the true kernel does [62]. The simplest such kernel (39), yielding two piecewise constant eigenfunctions (37) with opposite-sign eigenvalues, can be extended [129] such that interactions competing with the Coulomb repulsion are taken into account.

We consider a Fermi contour in the form of a hole pocket, which corresponds to perfect nesting in the case of pairing

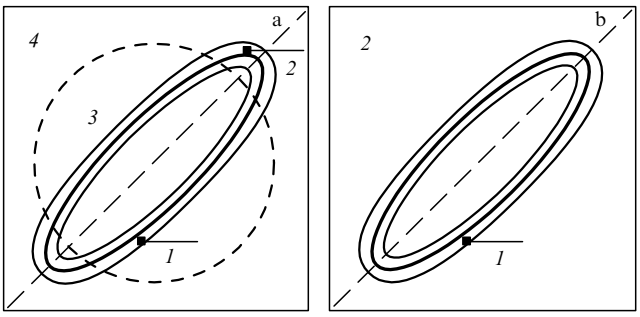

Figure 14. Competition between Coulomb pairing repulsion and EPI-induced attraction. Separation of the kinematically allowed region corresponding to a hole pocket: (a) for pairing repulsion of form (39); (b) for the BCS model [28]. The numbers indicate constant-sign regions of the superconducting order parameter.

with the momentum $\mathbf{K} = (\pi, \pi)$, and whose kinematically allowed region is a quarter of the Brillouin zone (Fig. 14). The Coulomb repulsion is defined in the entire kinematically allowed region, whereas the EPI-induced attraction is only significant in a narrow neighborhood of the Fermi contour with the energy width $\sim 2\hbar\omega_D$, where the contribution of the EPI attraction can be considered momentum-independent ($-V = \text{const}$).

The pairing Coulomb repulsion in (20) leads to the intersection of the line of zeros of $\Delta(\mathbf{k})$, which is a circle centered at the point $\mathbf{K}/2$, with the Fermi contour (see Fig. 6). Then, already in the absence of the EPI attraction, the kinematically allowed region is separated by this line into regions in which $\Delta(\mathbf{k})$ has opposite signs. Accordingly, in considering the EPI attraction, each of these regions is separated into parts in one of which (adjoining the Fermi contour) kernel (39) of the pairing Coulomb interaction should be supplemented with the contribution of the EPI attraction. If only a part of the Fermi contour belongs to the kinematically allowed region, the EPI attraction must be taken into account in the entire dynamically allowed region in the neighborhood of the entire Fermi contour. As a result, instead of two equations (38), we must write a system of four equations for each of the four regions Ξ_s ($s = 1, 2, 3, 4$) with constant (averaged over these regions) values Δ_s of the energy gap parameter $\Delta(\mathbf{k})$:

$$\begin{aligned} 2\Delta_1 &= +V\Delta_1 f_1 - (U-V)\Delta_2 f_2 - U\Delta_4 f_4\,, \\ 2\Delta_2 &= -(U-V)\Delta_1 f_1 + V\Delta_2 f_2 - U\Delta_3 f_3\,, \\ 2\Delta_3 &= -U\Delta_2 f_2 - U\Delta_4 f_4\,, \\ 2\Delta_4 &= -U\Delta_1 f_1 - U\Delta_3 f_3\,. \end{aligned} \tag{82}$$

Here, Δ_1 and Δ_2 are the respective average values of the energy gap parameter near the Fermi contour (in the EPI attraction region) inside and outside the circle $k = k_0$ and Δ_3 and Δ_4 are the order parameter values inside and outside the circle $k = k_0$ outside the EPI attraction region. For each of the Ξ_s regions, the quantities

$$f_s = \sum_{\mathbf{k}\in\Xi_s} \frac{1}{\sqrt{\xi^2(\mathbf{k}) + \Delta_s^2}} \tag{83}$$

can be estimated to logarithmic accuracy as

$$f_s = g \ln\left(\frac{2\hbar\omega_{\mathrm{D}}}{|\Delta_s|}\right), \qquad s = 1, 2;$$
$$f_s = g \ln\left(\frac{\varepsilon_0}{2\hbar\omega_{\mathrm{D}}}\right) \equiv f, \qquad s = 3, 4, \tag{84}$$

where g is the density of states and ε_0 is the energy scale of the kinematically allowed region, $\varepsilon_0 \gg \hbar\omega_{\mathrm{D}}$.

System of equations (82) can be reduced [129] to a system of two equations for Δ_1 and Δ_2:

$$\Delta_1 + w_0 f \Delta_2 = \gamma V [f_1 \Delta_1 + f_2 \Delta_2] - w_0 f_2 \Delta_2 ,$$
$$\Delta_2 + w_0 f \Delta_1 = \gamma V [f_1 \Delta_1 + f_2 \Delta_2] - w_0 f_1 \Delta_1 , \tag{85}$$

where $2w_0 = U$ and $\gamma = (1 + w_0 f)/2$.

The derived system of equation is invariant under the transformations $\Delta_1 \to -\Delta_2$ and $\Delta_1 \to \Delta_2$ and, therefore, has two solutions.

The asymmetric solution $\Delta_1 = -\Delta_2$ leads to $\Delta_3 \to \Delta_1$ and $\Delta_4 \to -\Delta_2$, where Δ_3 and Δ_4 are solutions of the system of self-consistency equations outside the EPI attraction band in the regions inside and outside the circle of zeros, respectively. In this case, the EPI coupling constant V drops out of the system of equations, and the only independent parameter characterizing the energy gap is

$$\Delta_1 = 2\varepsilon_0 \exp\left(-\frac{1}{g w_0}\right) \tag{86}$$

for any V.

The symmetric solution $\Delta_1 = \Delta_2$ is given by

$$\Delta_1 = 2\hbar\omega_{\mathrm{D}} \exp\left(-\frac{1}{g V^*}\right), \tag{87}$$

where $V^* = V - V_0$ with $V_0 = w_0/\left[1 + g w_0 \ln(\varepsilon_0/\hbar\omega_{\mathrm{D}})\right]$. Thus, a symmetric solution exists if $V > V_0$ in accordance with inequality (1). The energy gap parameters outside the EPI attraction band are equal to

$$\Delta_3 = \Delta_4 = -\frac{\Delta_1 w_0}{V\left[1 + g w_0 \ln(\varepsilon_0/\hbar\omega_{\mathrm{D}})\right] - w_0} . \tag{88}$$

For a weak EPI attraction, $V < V_0$, the pairing is due to the Coulomb repulsion with an asymmetric order parameter with an extended s-wave symmetry. The appearance of a symmetric solution for $V > V_0$ corresponds to an increase in the contribution of the isotropic component of the order parameter until its symmetry changes to an anisotropic s-wave symmetry (without zeros on the Fermi contour) for

$$V > \frac{2w_0}{1 - g^2 w_0^2 \left[\ln(\varepsilon_0/\hbar\omega_{\mathrm{D}})\right]^2} .$$

Figure 15a shows the diagram illustrating the competition between the pairing Coulomb repulsion and the EPI attraction. In a strongly correlated electron system, the Coulomb repulsion occurs in the case of a weak EPI (region I in the diagram), whereas in the opposite limit case (region III), the EPI attraction is observed, which can lead to the dominance of the Cooper (for $\mathbf{K} = 0$) channel of superconducting pairing as V increases. Transition region II corresponds to the competition between the Coulomb and EPI pairing channels.

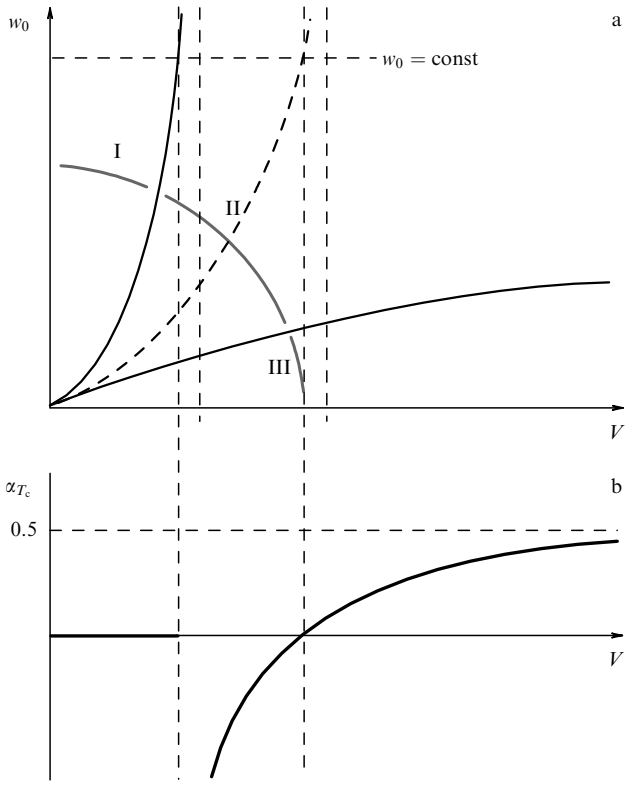

Figure 15. (a) Competition between the Coulomb pairing repulsion and the EPI attraction depending on the effective coupling constants w_0 and V. (b) Dependence of the isotope effect coefficient α_{T_c} on the EPI coupling constant V for $w_0 = \mathrm{const}$.

We note that if we assume the Coulomb repulsion to be constant in the entire kinematically allowed region ($U_{\mathrm{C}} = \mathrm{const}$) and the contribution of the EPI attraction to be nonzero and constant in the neighborhood of the Fermi contour, that is, if we choose elements of the piecewise constant kernel in the system of self-consistency equations (82) as $U_{11} = U_{\mathrm{C}} - V$, $U_{12} = U_{21} = U_{22} \equiv U_{\mathrm{C}}$ (subscript 1 refers to the neighborhood of the Fermi contour in which the EPI attraction is substantial and subscript 2 refers to the remaining part of the kinematically allowed region, Fig. 14b), then a nontrivial solution exists under the known [28] restriction (1) on the EPI attraction constant and determines the value above which the superconducting pairing is possible. With this assumption concerning the form of the elements $U_{ss'}$ of the degenerate kernel, the solution of system of equations (38) specifies the energy gap parameter that has opposite signs in the regions Ξ_1 and Ξ_2. Thus, $\Delta(\mathbf{k})$ has lines of zeros coincident with the boundary of the EPI attraction region, i.e., not intersecting the Fermi contour [129].

The antiferromagnetic magnon exchange can also be taken into account within the semi-phenomenological scheme based on the system of self-consistency equations (38). For the Fermi contour in the form of four hole pockets, the coupling constants for such a pairing interaction correspond to repulsion for scattering inside a pocket and between pockets along the diagonal of the Brillouin zone and to attraction for scattering between nearest-neighbor pockets. The interaction due to the antiferromagnetic magnon exchange has a rather weak effect on the magnitude of the energy gap parameter, which is mainly determined by the

Coulomb pairing. However, for certain relations between the coupling constants, this interaction can cause a change in the order parameter symmetry from the extended s-wave to the d-wave symmetry with additional (associated with the Coulomb repulsion from large-momentum pairing) zeros on the Fermi contour.

23. Isotope effect

The pairing caused by the EPI repulsion leads to a universal dependence of the superconducting transition temperature and other superconductor characteristics on its isotopic composition. The isotope effect index for T_c,

$$\alpha_{T_c} = -\frac{\mathrm{d}\ln T_c}{\mathrm{d}\ln M} = \frac{1}{2}\frac{\mathrm{d}\ln \Delta}{\mathrm{d}\ln 2\hbar\omega_D}\,, \tag{89}$$

is then equal to 0.5. Here, M is the atomic mass that changes under the isotope substitution.

In cuprate superconductors, the best investigated effect is that of the oxygen isotope substitution $^{16}O \to {}^{18}O$ [130–133]. In optimally doped compounds, α_{T_c} deviates from the value 0.5 that is universal for the EPI superconductivity mechanism. This value increases with decreasing doping.

Small (close to zero) α values imply that the dominant mechanism of cuprate superconductivity is the Coulomb pairing, which corresponds to the strictly zero isotope effect index. However, nonzero doping-dependent α_{T_c} values, as well as the observation of the so-called negative isotope effect [134], suggest that the EPI contribution to the superconducting pairing in cuprates is not negligibly small [37, 135, 136].

Because the superconducting pairing in cuprates occurs in cuprate planes with approximately equal parameters for all cuprate compounds [18], it is natural to believe that the Coulomb coupling constant w_0 is also approximately the same for all such compounds. Using the obtained expressions (86) and (87) for the energy gap, we can verify that in region I, corresponding to the weak EPI coupling (Fig. 15a), we have $\alpha_{T_c} = 0$, whereas in regions III (with the strong EPI coupling) and II (corresponding to the transition from the extended to anisotropic s-wave symmetry of the order parameter), the isotope effect index is given by

$$\alpha_{T_c} = \frac{1}{2}\left[1 - \left(\frac{w_0}{V\left[1 + g w_0 \ln\left(\varepsilon_0/\hbar\omega_D\right)\right] - w_0}\right)^2\right]. \tag{90}$$

The dependence $\alpha_{T_c}(V)$ for $w_0 = \text{const}$ is given in Fig. 15b. The index $\alpha_{T_c} \to 0.5$ as $V/w_0 \to \infty$ and is negative for $V_0 < V < 2V_0$.

The values of the isotope effect indices in the same cuprate compound for different doping levels can be different because a change in the chemical composition results in the corresponding change in the effective coupling constants U and V, and (which is perhaps most important) in the density of states g of the relative pair motion, which is proportional to the Fermi contour length within the kinematically allowed region.

24. Conclusion

Strong Coulomb correlations in quasi-two-dimensional parent cuprates, leading to a spin antiferromagnetic insulating ground state and manifesting themselves as a short-range order in doped compounds, play a decisive role in the formation of the electron structure of cuprates. The Fermi contour of doped cuprates observed in experiments on photoemission is located in extended neighborhoods of the saddle points of the electron dispersion law. The approximate mirror nesting of finite regions of the Fermi contour for pairs of particles with a large total momentum $\mathbf{K}$ equal or close to the vector of the reciprocal lattice of the antiferromagnetic parent compound occurs in a rather wide doping range in the region of the superconducting ground state.

A logarithmic singularity of the scattering amplitude of two interacting particles with a total momentum $\mathbf{K}$ corresponds to perfect nesting, not only in the pairing attraction (as in the Cooper problem for $\mathbf{K} = 0$) but also in the screened Coulomb repulsion, which can thus be considered the fundamental pairing interaction determining both the insulating and superconducting states of cuprates. In the case of approximate mirror nesting, the superconducting pairing with $\mathbf{K} \neq 0$ is possible if the effective coupling constant exceeds a certain value, which increases with the deviation from the ideal mirror nesting.

Because of the kinematic restriction that holds for pairing with $\mathbf{K} \neq 0$, the screened Coulomb repulsion also allows weakly damping quasistationary states of incoherent pairs, which can exist in a wide temperature range (~ 100 K) of a strong pseudogap corresponding to developed fluctuations of the superconducting order parameter.

If mirror nesting holds not on the entire Fermi contour but only on its part, not all the particles precipitate to the superconducting condensate and the two-fluid behavior persists to the lowest temperatures and is displayed in the Drude component of optical conductivity (observed at $T < T_c$) corresponding to more than half the free carriers. In underdoped cuprates, the Fermi contour shows up as hole pockets with the perfect mirror and ordinary nesting with the momentum corresponding to the antiferromagnetic vector of the parent composition. As a result of weakening of antiferromagnetic correlations, half of the hole pocket, pertaining to the main band, preserves the weakly doping-dependent spectral intensity, while the other half, corresponding to the shadow band, gradually attenuates with increasing doping. The probability of pairing with $\mathbf{K} \neq 0$ of a carrier from the main band with a carrier from the shadow zone is determined by the occupation of the latter. The difference in occupations of the main and shadow bands is equal to the fraction of carriers outside the superconducting condensate, characterizing the Drude component of the optical conductivity at $T < T_c$. Similar behavior of the particles outside the condensate at $T < T_c$ is observed in the temperature dependence of thermal capacity: $C_V \sim \gamma T$ [137].

In Ginzburg–Landau-type macroscopic equations, the relative phase of a two-component superconducting order parameter manifests itself as an orbital current degree of freedom of the relative motion of a pair. This allows a phase transition inside the superconducting state. One of the superconducting phases corresponds to the coexistence of superconductivity and circular orbital currents (bound vortex–antivortex pairs), while the other phase (corresponding to higher doping levels) represents a spatially inhomogeneous condensate of pairs of particles with the momentum $\mathbf{K} \neq 0$. The study of nonuniform order parameter component distributions within the model in [90] shows [138, 139] that the occurrence of current states in a system of strongly correlated electrons with a large (as distinct from the FFLO state) total pair momentum is accompanied by a decrease in the free energy.

In the underdoped part of the superconducting region, the main state competing with superconductivity and existing above T_c up to the weak-pseudogap temperature T^* is the insulating state with an orbital antiferromagnetic order. The pseudogap state displays diamagnetic behavior strengthened in the region of developed superconducting fluctuations (strong pseudogap) and manifests itself as a nonlinear Meissner effect. The superconducting order parameter as a function of the momentum of the relative motion of a pair in pairing repulsion has the line of zeros crossing the Fermi contour in the kinematically allowed region. Therefore, the line of zeros of the quasiparticle group velocity does not coincide with the Fermi contour, which explains some of the observed specific features of superconducting cuprates, namely, the weak Andreev reflection, the asymmetry of the tunnel volt – ampere characteristics, and the 'peak – dip – hump' structure of the tunnel and photoemission spectra.

The very existence of the line of zeros of a superconducting order parameter is associated with the predominant pairing-induced Coulomb repulsion. The interactions due to the phonon or antiferromagnetic magnon exchange not only affect the position of this line and the superconducting gap amplitude but also determine the relations between the order-parameter phases for each of the crystal-equivalent momenta **K**. This determines the observed symmetry of the superconducting gap, as well as specific manifestations of the isotope effect and the low sensitivity to scattering by nonmagnetic impurities in cuprates.

This work was supported by the Russian Foundation for Basic Research (grant 05-02-17077a and 06-02-17186a).

References

1. Bednorz J G, Müller K A *Z. Phys. B* **64** 189 (1986)
2. Anderson P W *Science* **235** 1196 (1987)
3. Takigawa M et al. *Phys. Rev. B* **39** 7371 (1989)
4. Cooper L N *Phys. Rev.* **104** 1189 (1956)
5. Bardeen J, Cooper L N, Schrieffer J R *Phys. Rev.* **108** 1175 (1957)
6. Sachdev S *Science* **288** 475 (2000)
7. Zhang S-C *Science* **275** 1089 (1997)
8. Guidry M et al. *Phys. Rev. B* **63** 134516 (2001)
9. Nayak C *Phys. Rev. B* **62** 4880 (2000)
10. Carlson E W et al., in *The Physics of Superconductors* Vol. 2 (Eds K-H Bennemann, J B Ketterson) (Berlin: Springer-Verlag, 2004) (in press); cond-mat/0206217
11. Klemm R A *Int. J. Mod. Phys. B* **12** 2920 (1998)
12. Tsuei C C, Kirtley J R *Rev. Mod. Phys.* **72** 969 (2000)
13. Zhao G *Phys. Rev. B* **64** 024503 (2001)
14. Brandow B H *Phys. Rev. B* **65** 054503 (2002)
15. Belyavskĭ V I, Kopaev Yu V *Usp. Fiz. Nauk* **174** 457 (2004) [*Phys. Usp.* **47** 409 (2004)]
16. Orenstein J, Millis A J *Science* **288** 468 (2000)
17. Lee P A, Nagaosa N, Wen X-G *Rev. Mod. Phys.* **78** 17 (2006)
18. Dagotto E *Rev. Mod. Phys.* **66** 763 (1994)
19. Gofron K et al. *Phys. Rev. Lett.* **73** 3302 (1994)
20. Shen Z-X et al. *Science* **267** 343 (1995)
21. Fujimori A et al. *Physica C* **341 – 348** 2067 (2000)
22. Norman M R et al. *Nature* **392** 157 (1998); Coleman P *Nature* **392** 134 (1998)
23. Basov D N, Timusk T *Rev. Mod. Phys.* **77** 721 (2005)
24. Chubukov A V, Pines D, Schmalian J, in *The Physics of Superconductors* Vol. 1 (Eds K-H Bennemann, J B Ketterson) (Berlin: Springer-Verlag, 2003) p. 495; cond-mat/0201140
25. Wang Y et al. *Phys. Rev. Lett.* **95** 247002 (2005); cond-mat/0503190
26. Xu Z A et al. *Nature* **406** 486 (2000)
27. Vedeneev S I, Maude D K *Phys. Rev. B* **72** 214514 (2005)
28. Bogolyubov N N, Tolmachev V V, Shirkov D V *Novyi Metod v Teorii Sverkhprovodimosti* (A New Method in the Theory of Superconductivity) (Moscow: Izd. AN SSSR, 1958) [Translated into English (New York: Consultants Bureau, 1959)]
29. Moskalenko V A *Fiz. Met. Metalloved.* **8** 503 (1959) [*Phys. Met. Metallogr.* **8** 25 (1959)]
30. Suhl H, Matthias B T, Walker L R *Phys. Rev. Lett.* **3** 552 (1959)
31. Kohn W, Luttinger J M *Phys. Rev. Lett.* **15** 524 (1965)
32. Baz' A I, Zel'dovich Ya B, Perelomov A M *Rasseyanie, Reaktsii i Raspady v Nerelyativistskoi Kvantovoi Mekhanike* (Scattering, Reactions and Decay in Nonrelativistic Quantum Mechanics) 2nd ed. (Moscow: Nauka, 1971) [Translated into English (Jerusalem: Israel Program for Scientific Translations, 1969)]
33. Lifshitz E M, Pitaevskii L P *Statisticheskaya Fizika* (Statistical Physics) Pt. 2 (Moscow: Fizmatlit, 2001) [Translated into English (Oxford: Pergamon Press, 1980)]
34. Mineev V P, Samokhin K V *Vvedenie v Teoriyu Neobychnoi Sverkhprovodimosti* (Introduction to Unconventional Superconductivity) (Moscow: Izd. MFTI, 1998) [Translated into English (Amsterdam: Gordon and Breach Sci. Publ., 1999)]
35. Ziman J M *Principles of the Theory of Solids* 2nd ed. (Cambridge: Univ. Press, 1972) [Translated into Russian (Moscow: Mir, 1974)]
36. Kagan M Yu, Chubukov A V *Pis'ma Zh. Eksp. Teor. Fiz.* **47** 525 (1988) [*JETP Lett.* **47** 614 (1988)]
37. Maksimov E G *Usp. Fiz. Nauk* **170** 1033 (2000) [*Phys. Usp.* **43** 965 (2000)]
38. Berk N F, Schrieffer J R *Phys. Rev. Lett.* **17** 433 (1966)
39. Izyumov Yu A *Usp. Fiz. Nauk* **169** 225 (1999) [*Phys. Usp.* **42** 215 (1999)]
40. Kuroki K, Arita R *Phys. Rev. B* **64** 024501 (2001)
41. Yang C N *Phys. Rev. Lett.* **63** 2144 (1989)
42. Penson K A, Kolb M *Phys. Rev. B* **33** 1663 (1986)
43. Robaszkiewicz S, Bulka B R *Phys. Rev. B* **59** 6430 (1999)
44. Japaridze G I et al. *Phys. Rev. B* **65** 014518 (2002)
45. Fulde P, Ferrell R A *Phys. Rev.* **135** A550 (1964)
46. Larkin A I, Ovchinnikov Yu N *Zh. Eksp. Teor. Fiz.* **47** 1136 (1964) [*Sov. Phys. JETP* **20** 762 (1965)]
47. Belyavsky V I, Kapaev V V, Kopaev Yu V *Zh. Eksp. Teor. Fiz.* **118** 941 (2000) [*JETP* **91** 817 (2000)]
48. Belyavsky V I, Kopaev Yu V *Pis'ma Zh. Eksp. Teor. Fiz.* **73** 87 (2001) [*JETP Lett.* **73** 82 (2001)]
49. Belyavsky V I, Kopaev Yu V *Phys. Rev. B* **67** 024513 (2003)
50. Belyavsky V I, Kopaev Yu V, Sofronov V M, Shevtsov S V *Zh. Eksp. Teor. Fiz.* **124** 1149 (2003) [*JETP* **97** 1032 (2003)]
51. Belyavsky V I, Kapaev V V, Kopaev Yu V *Pis'ma Zh. Eksp. Teor. Fiz.* **76** 51 (2002) [*JETP Lett.* **76** 44 (2002)]
52. Kopaev Yu V, Sofronov V M *Phys. Lett. A* **344** 297 (2005)
53. Krasnov M L *Integral'nye Uravneniya* (Integral Equations) (Moscow: Nauka, 1967)
54. Kirzhnits D A, in *Problema Vysokotemperaturnoi Sverkhprovodimosti* (The Problem of High-Temperature Superconductivity) (Eds V L Ginzburg, D A Kirzhnits) (Moscow: Nauka, 1977) Ch. 2 [Translated into English: in *High-Temperature Superconductivity* (Eds V L Ginzburg, D A Kirzhnits) (New York: Consultants Bureau, 1982)]
55. Yang K, Sondhi S L *Phys. Rev. B* **62** 11778 (2000)
56. Belyavskii V I, Kopaev Yu V, Togushova Yu N, Shevtsov S V *Zh. Eksp. Teor. Fiz.* **126** 672 (2004) [*JETP* **99** 585 (2004)]
57. Fikhtengol'ts G M *Kurs Differentsial'nogo i Integral'nogo Ischisleniya* (Course in Differential and Integral Calculus) Vol. 2 (Moscow: Fizmatlit, 1962) [Translated into English: Fichtenholz G M *Infinite Series: Rudiments* (New York: Gordon and Breach, 1970)]
58. Emery V J, Kivelson S A *Nature* **374** 434 (1995)
59. Eliashberg G M *Zh. Eksp. Teor. Fiz.* **38** 966; **39** 1437 (1960) [*Sov. Phys. JETP* **11** 696 (1960); **12** 1000 (1961)]
60. Abrikosov A A *Phys. Rev. B* **63** 134518 (2001)
61. Chiao M et al. *Phys. Rev. B* **62** 3554 (2000)
62. Belyavsky V I, Kopaev Yu V, Togushova Yu N *Phys. Lett. A* **338** 69 (2005)
63. Chakravarty S et al. *Phys. Rev. B* **63** 094503 (2001)
64. Oda M et al. *Physica* C **341 – 348** 847 (2000)
65. Campuzano J C, Norman M R, Randeria M, in *The Physics of Superconductors* Vol. 2 (Eds K-H Bennemann, J B Ketterson) (Berlin: Springer-Verlag, 2004) (in press); cond-mat/0209476
66. Damascelli A, Hussain Z, Shen Z-X *Rev. Mod. Phys.* **75** 473 (2003)

67. Kampf A, Schrieffer J R *Phys. Rev. B* **42** 7967 (1990)
68. Liechtenstein A I et al. *Phys. Rev. B* **54** 12505 (1996)
69. Freeman A J, Yu J *Helv. Phys. Acta* **61** 401 (1988)
70. Pickett W E et al. *Science* **255** 46 (1992)
71. Lifshits I M *Zh. Eksp. Teor. Fiz.* **38** 1569 (1960) [*Sov. Phys. JETP* **11** 1130 (1960)]
72. Belyavsky V I, Kapaev V V, Kopaev Yu V *Pis'ma Zh. Eksp. Teor. Fiz.* **81** 650 (2005) [*JETP Lett.* **81** 527 (2005)]
73. Sadovskiĭ M V *Usp. Fiz. Nauk* **171** 539 (2001) [*Phys. Usp.* **44** 515 (2001)]
74. Chakravarty S, Nayak C, Tewari S *Phys. Rev. B* **68** 100504(R) (2003); cond-mat/0306084
75. Ino A et al. *Phys. Rev. B* **62** 4137 (2000)
76. Morgan B et al., cond-mat/0512459
77. Boebinger G S et al. *Phys. Rev. Lett.* **77** 5417 (1996)
78. Belyavsky V I, Kopaev Yu V, Smirnov M Yu *Zh. Eksp. Teor. Fiz.* **128** 525 (2005) [*JETP* **101** 452 (2005)]
79. Scalapino D J, Loch E (Jr), Hirsch J E *Phys. Rev. B* **35** 6694 (1987)
80. Belyavsky V I, Kopaev Yu V *Zh. Eksp. Teor. Fiz.* **127** 45 (2005) [*JETP* **100** 39 (2005)]
81. Kotegawa H et al. *J. Phys. Chem. Solids* **62** 171 (2001)
82. Scott B A et al. *Physica C* **230** 239 (1994)
83. Kuzemskaya I G, Kuzemsky A L, Cheglokov A A *J. Low-Temp. Phys.* **118** 147 (2000)
84. Chakravarty S, Kee H-Y, Völker K *Nature* **428** 53 (2004)
85. Ren Y, Xu J-H, Ting C S *Phys. Rev. Lett.* **74** 3680 (1995)
86. Ghosh A, Adhikari S K *Phys. Rev. B* **60** 10401 (1999)
87. Shimahara H *J. Phys. Soc. Jpn.* **67** 1872 (1998); cond-mat/0406384
88. Hardy W N et al. *Phys. Rev. Lett.* **70** 3999 (1993)
89. Lee P A, Wen X-G *Phys. Rev. Lett.* **78** 4111 (1997)
90. Babaev E, Faddeev L D, Niemi A J *Phys. Rev. B* **65** 100512 (2002)
91. Ivanov D A, Lee P A, Wen X-G *Phys. Rev. Lett.* **84** 3958 (2000)
92. Lee P A et al. *Phys. Rev. B* **57** 6003 (1998); Lee P A, cond-mat/0201052
93. Weng Z Y, Sheng D N, Ting C S *Phys. Rev. B* **59** 8943 (1999)
94. Muthukumar V N, Weng Z Y *Phys. Rev. B* **65** 174511 (2002)
95. Zhou S, Wang Z *Phys. Rev. B* **70** 020501 (2004); cond-mat/0401436
96. Affleck I, Marston J B *Phys. Rev. B* **37** 3774 (1988)
97. Volkov B A, Gorbatsevich A A, Kopaev Yu V, Tugushev V V *Zh. Eksp. Teor. Fiz.* **81** 729 (1981) [*Sov. Phys. JETP* **54** 391 (1981)]
98. Ginzburg V L, Gorbatsevich A A, Kopayev Yu V, Volkov B A *Solid State Commun.* **50** 339 (1984)
99. Varma C M *Phys. Rev. B* **55** 14554 (1997); *Phys. Rev. Lett.* **83** 3538 (1999); cond-mat/0507214
100. Kaminski A et al. *Nature* **416** 610 (2002)
101. Fauque B et al., cond-mat/0509210
102. Armitage N P, Hu J, cond-mat/0303186; Kaminski A et al., cond-mat/0306140
103. Belyavsky V I, Kopaev Yu V, Smirnov M Yu *Phys. Rev. B* **72** 132501 (2005)
104. Corson J et al. *Nature* **398** 221 (1999)
105. Wang Y et al. *Science* **299** 86 (2003)
106. Anderson P W et al. *Phys. Rev. Lett.* **58** 2790 (1987)
107. Franz M, Tešanović Z, Vafek O *Phys. Rev. B* **66** 054535 (2002)
108. Chakravarty S *Phys. Rev. B* **66** 224505 (2002)
109. Landau L D, Lifshitz E M *Elektrodinamika Sploshnykh Sred* (Electrodynamics of Continuous Media) (Moscow: Nauka, 1992) [Translated into English (Oxford: Pergamon Press, 1984)]
110. Kopaev Yu V *Fiz. Tverd. Tela* **12** 3 (1970)
111. Rice T M *Phys. Rev. B* **2** 3619 (1970)
112. Sarma G *J. Phys. Chem. Solids* **24** 1029 (1963)
113. Gor'kov L P, Rusinov A I *Zh. Eksp. Teor. Fiz.* **46** 1363 (1964) [*Sov. Phys. JETP* **19** 922 (1964)]
114. Glover R E (III), Tinkham M *Phys. Rev.* **104** 844 (1956); **108** 243 (1957)
115. Ferrell R A, Glover R E (III) *Phys. Rev.* **109** 1398 (1958)
116. Tinkham M, Ferrell R A *Phys. Rev. Lett.* **2** 331 (1959)
117. Basov D N et al. *Science* **283** 49 (1999); Klein M V, Blumberg G *Science* **283** 42 (1999)
118. Hirsch J E, Marsiglio F *Phys. Rev. B* **62** 15131 (2000)
119. Norman M R et al. *Phys. Rev. B* **61** 14742 (2000)
120. Uemura Y J et al. *Phys. Rev. Lett.* **66** 2665 (1991)
121. Homes C C et al. *Nature* **430** 539 (2004)
122. Landau L D, Lifshitz E M *Statisticheskaya Fizika* (Statistical Physics) Pt. 1 (Moscow: Fizmatlit, 2002) [Translated into English (Oxford: Pergamon Press, 1980)]
123. Hirsch J E *Physica C* **341–348** 213 (2000)
124. Hirsch J E *Phys. Rev. B* **59** 11962 (1999)
125. Andreev A F *Zh. Eksp. Teor. Fiz.* **46** 1823 (1964) [*Sov. Phys. JETP* **19** 1228 (1964)]
126. Deutscher G *Rev. Mod. Phys.* **77** 109 (2005)
127. Kopaev Yu V, Sofronov V M *Pis'ma Zh. Eksp. Teor. Fiz.* **82** 652 (2005) [*JETP Lett.* **82** 575 (2005)]
128. Blonder G E, Tinkham M, Klapwijk T M *Phys. Rev. B* **25** 4515 (1982)
129. Belyavsky V I, Kopaev Yu V, Nguyen N T, Togushova Yu N *Phys. Lett. A* **342** 267 (2005)
130. Zhao G, Singh K K, Morris D E *Phys. Rev. B* **50** 4112 (1994)
131. Zhao G et al. *Nature* **385** 236 (1997)
132. Pringle D J, Williams G V M, Tallon J L *Phys. Rev. B* **62** 12527 (2000)
133. Williams G V M et al. *Phys. Rev. Lett.* **80** 377 (1998)
134. Franck J P, Lawrie D D *J. Supercond.* **8** 591 (1995)
135. Abrikosov A A *Physica C* **341–348** 97 (2000)
136. Zhao G et al. *Phys. Rev. B* **54** 14956 (1996)
137. Loram J W et al. *Physica* C **341-348** 831 (2000)
138. Isaev L S, Protogenov A P *Zh. Eksp. Teor. Fiz.* **123** 1297 (2003) [*JETP* **96** 1140 (2003)]
139. Protogenov A P *Usp. Fiz. Nauk* **176** 689 (2006) [*Phys. Usp.* **49** (7) (2006)]